

September 12, 2011

Craig Hoffman
Compliance Project Manager
California Energy Commission
1516 Ninth Street, MS-2000
Sacramento, CA 95814

DOCKET	
08-AFC-13C	
DATE	SEP 12 2011
RECD.	SEP 12 2011

Subject: Calico Solar 08-AFC-13C
Calico Solar Project Geomorphic Report

Dear Mr. Hoffman:

K Road Calico Solar LLC hereby submits the Calico Solar Project Geomorphic and Hydraulic Analysis and Geomorphic and Biologic Analysis Report dated September 12, 2011. I certify under penalty of perjury that the foregoing is true, correct and complete to the best of my knowledge.

Sincerely,



Daniel J. O'Shea
On behalf of K Road Calico Solar, LLC
formerly known as Calico Solar, LLC

Calico Solar Project

Geomorphic and Hydraulic Analysis and Geomorphic and Biologic Analysis Report



Submitted to: **K Road Calico Solar LLC**
2600 Tenth Street, Suite 635
Berkeley, California 94107



Submitted by:  **TETRA TECH**
3801 Automation Way, Suite 100
Fort Collins, Colorado 80525

September 12, 2011

Table of Contents

	<u>Page</u>
1 INTRODUCTION AND BACKGROUND	1.1
1.1 Soil and Water Conditions Require a Geomorphic and Hydraulics Analysis and a Geomorphic and Biologic Analysis	1.1
1.2 Authorization and Project Team	1.3
2 GEOMORPHIC SETTING AND SEDIMENT-TRANSPORT PROCESSES	2.1
2.1 Climate and Precipitation.....	2.1
2.1.1 General.....	2.1
2.1.2 Effects of El Niño and La Niña	2.7
2.2 Soil, Vegetation, and Erodibility Factors	2.10
3 SITE HYDROLOGY AND HYDRAULIC ANALYSIS	3.1
3.1 Existing Conditions Model	3.1
3.2 Proposed Conditions Model	3.1
3.3 Model Results.....	3.9
3.3.1 Existing Conditions	3.9
3.3.2 Proposed Conditions	3.14
4 SEDIMENT-TRANSPORT ANALYSIS TO ADDRESS GEOMORPHIC AND BIOLOGIC ISSUES.....	4.1
5 SUMMARY AND CONCLUSIONS	5.1
6 REFERENCES	6.1
APPENDIX A: Proposed Conditions Hydraulics	A.1

List of Figures

Figure 1.1. Map of the Calico Solar project site and watersheds.	1.2
Figure 2.1. Topographic surface of the project site and upstream watershed.....	2.2
Figure 2.2. Topographic slopes at the project site and upstream watersheds.	2.3
Figure 2.3. Typical view of the bajada surface covered by the Mojave creosote bush scrub vegetation community and Cady Mountains from southeast corner of Section 4 near the extension of Hector Road.....	2.4
Figure 2.4. View looking downstream in the wash below BNSF Railroad Drainage Structure No. 4, near the center of Section 4 (see Figure 2.2 for location). Much of the fine sand that is visible in this photograph is a veneer of Aeolian origin over the coarser underlying alluvial sand.	2.5
Figure 2.5. Average monthly precipitation from 1948 through 2010 at Daggett FAA Airport.....	2.6

Figure 2.6.	Oceanic Niño Index (ONI) for period from 1950 through mid-2011. Warm period corresponding to El Niño and La Nina conditions are defined as 5 consecutive overlapping tri-monthly periods exceeding ± 0.5 , respectively (i.e., El Niño >0.5 , La Niña <0.5) (from NOAA, 2011)	2.8
Figure 2.7.	Relationship between total winter wet season (October through March) precipitation and Oceanic Niño Index (ONI) based on data from Daggett FAA Airport station.	2.9
Figure 2.8.	Hydrologic soil groups in the vicinity of the project from NRCS STATSGO2 website.	2.11
Figure 2.9.	Geology map of the vicinity of the project site.	2.13
Figure 2.10.	Aerial photograph (June 14, 2009) of watershed showing the bedrock and alluvial surfaces.	2.14
Figure 2.11a.	Location of surface sediment samples collected by Tetra Tech (2011) and URS (2009).	2.15
Figure 2.11b.	Particle size distribution curves for samples collected by Tetra Tech (2011)...	2.15
Figure 2.12.	View looking downstream in a well-defined wash along north boundary of the Project site near Sample S4 showing the typical surface bed material characteristics.	2.16
Figure 2.13.	Particle size distribution curves for three near-surface sediment samples collected by URS (2009).	2.16
Figure 2.14.	View looking NE across the bajada/fan surface toward to Cady Mountains showing the typical Mojave creosote bush scrub community.	2.17
Figure 3.1.	Map of project site and contributing drainage subbasins showing the locations of the FLO-2D inflow nodes for the off-site basins and the BNSF railroad crossings.	3.4
Figure 3.2.	Project site map showing features under full build-out conditions.	3.6
Figure 3.3.	Typical PV panel layout (A=171 feet, B=19.6 feet, C=281 feet, X=3.4 feet, Y=6.5 feet).	3.8
Figure 3.4.	Photo of typical SunCatchers™.	3.9
Figure 3.5a.	Predicted maximum depth during 100-year, 24-hour storm under existing conditions.	3.12
Figure 3.5b.	Predicted maximum velocity during 100-year, 24-hour storm under existing conditions.	3.13
Figure 3.6a.	Predicted maximum depth during 100-year, 24-hour storm under full build-out conditions.	3.15
Figure 3.6b.	Predicted maximum velocity during 100-year, 24-hour storm under full build-out conditions.	3.16
Figure 3.7.	100-year, 24-hour storm hydrographs at Trestle 5 under existing and full build-out conditions. NOTE: Existing and proposed discharges are nearly identical; thus, existing discharge line is covered by proposed discharge line.	3.17

Figure 3.8.	100-year, 24-hour storm hydrographs at Trestle 6 under existing and full build-out conditions. NOTE: Existing and proposed discharges are nearly identical; thus, existing discharge line is covered by proposed discharge line.	3.17
Figure 4.1.	Bed-material sediment gradations used in the sediment-transport analysis.	4.2
Figure 4.2.	Location of sediment-transport analysis points and particle size gradation applied to each location.	4.3
Figure 4.3.	Graph showing the relation between sediment yield and drainage area for drainage basins in five different locations. Note that the Mojave Desert drainage basins generate an order of magnitude less sediment per unit area than basins elsewhere (modified from Griffiths et al., 2006).	4.5
Figure 4.4.	Comparison of total bed-material sediment loads for the 2- through 100-year storm hydrographs in the washes just upstream from the BNSF Railroad line (AP 77, AP 48, AP 52, AP 53, AP 59 and AP 60). Points falling below the red line indicate a decrease in sediment load under proposed conditions; points above the line indicate an increase in sediment load.	4.6
Figure 4.5.	Comparison of total bed-material sediment loads for the 2- through 100-year storm hydrographs in the washes at the analysis points shown in Figure 4.2 (except those shown in Figure 4.4). Points falling below the red line indicate a decrease in sediment load under proposed conditions; points above the line indicate an increase in sediment load.	4.7

List of Tables

Table 2.1.	Approximate point precipitation depths (inches) for the watershed at the project site.	2.7
Table 2.2.	Description of soils in the Project watersheds from NRCS STATSGO2 mapping (see Figure 3).	2.12
Table 3.1.	Peak discharges (cfs) at the FLO-2D inflow nodes for the 2-, 5-, 10-, 25-, 50- and 100-year storms under existing conditions.	3.2
Table 3.2.	Runoff volumes (ac-ft) at the FLO-2D inflow nodes for the 2-, 5-, 10-, 25-, 50- and 100-year storms under existing conditions.	3.3
Table 3.3.	FLO-2D hydrologic parameters.	3.5
Table 3.4.	FLO-2D results summary for the 6-hour storm event.	3.10
Table 3.5.	FLO-2D results summary for the 24-hour storm event.	3.11
Table 3.6.	Summary of predicted overtopping of the railroad line under existing conditions.	3.14

1 INTRODUCTION AND BACKGROUND

On December 1, 2010, the California Energy Commission (Commission) issued a decision (Commission Decision) approving and licensing the Calico Solar Project (Project) that would be owned and operated by K Road Calico Solar LLC (Calico). The Project site is located on 4,613 acres of land in San Bernardino County, California, that are primarily administered by the Bureau of Land Management (BLM) [Figure 1.1]. The Approved Project has a generating capacity of 663.5 megawatts (MW) that would be produced by solar collectors called “SunCatchers™.” Each of these solar collectors would consist of an approximately 38-foot-diameter mirrored dish and a Stirling engine, utilizing an internal working fluid of hydrogen gas. On March 22, 2011, Calico filed a petition with the Commission requesting to modify the Project to generate the same 663.5 MW capacity, but with 100.5 MW derived from SunCatchers™ technology and 563 MW derived from single-axis tracker photovoltaic (PV) technology. The overall project footprint for the Proposed Project is the same as for the Approved Project.

1.1 Soil and Water Conditions Require a Geomorphic and Hydraulics Analysis and a Geomorphic and Biologic Analysis

The Commission issued Soil & Water Conditions of Certification for the Approved Project. These conditions require, in-part, that Calico prepare a basis of design report that includes a geomorphic and hydraulic analysis *to determine the maximum design storm that can be routed through the site utilizing existing fluvial washes that will not result in significant damage to proposed site infrastructure and determine the ability of the proposed site infrastructure to withstand the storm at the proposed location of said site infrastructure. The result of this analysis shall not conflict with the requirement that the project not contribute to any impacts to the BNSF right of way due to a 100-year storm. (Soil&Water-8, Para 4.b.).*

Soil&Water-8 (Para 4.d.) also specifies that the basis of design report shall include a *geomorphic and biologic analysis to determine the minimum design storm that can be routed through the site utilizing existing fluvial washes that will provide the necessary sediment load through the site and "downstream areas" to maintain existing sensitive habitat needs, as described in the Geomorphic Assessment of Calico Solar Project Site. This analysis must consider and address the need for fine sand to support the existing sensitive habitat and the potential episodic nature of the associated dune complex evolution that depends upon El Niño events (i.e., wet winters occurring approximately every three to seven years) delivering sediment to the lower fan and the accompanying La Nina events (i.e., dry winters occurring approximately every three to seven years) eroding and transporting fine sands to these dunes through wind action.*

In addition, **Soil&Water-8 (Para 4.e.)** requires a *determination of the pass through design storm that can be routed through the site unimpeded to deliver the necessary sediment load through the site to maintain existing sensitive habitat needs in "downstream areas" and not result in significant damage to proposed site infrastructure.*

The Geomorphic Assessment that is referred to in Para 4.d. was prepared for the Commission by Phillip Williams & Associates, Ltd (PWA, 2010). This assessment focuses primarily on the physical processes that form and maintain aeolian sand dunes that are considered critical habitat for the Mojave Fringe-toed Lizard (MFTL). PWA (2010) concluded that the existing MFTL dune habitat is formed and maintained by alluvial sediment that is primarily brought onto the site by the washes during surface-runoff events and delivered to the dune

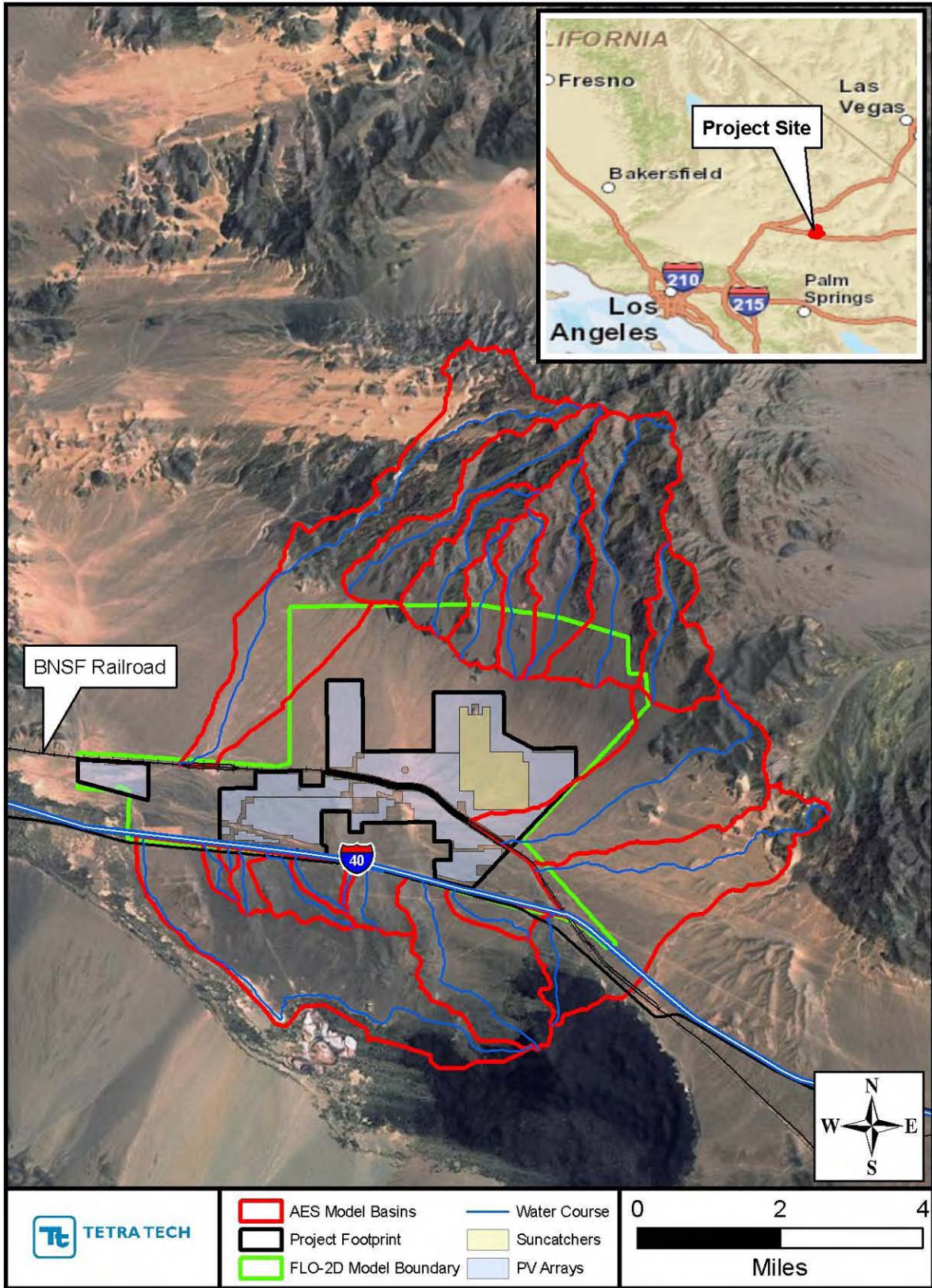


Figure 1.1. Map of the Calico Solar Project site and watersheds.

habitat through aeolian (i.e., wind) entrainment and transport from the washes; thus, the surface sediment supply must be maintained to, and through, the site to protect the habitat.

Notwithstanding the above conditions, it is important to understand that the overall sediment load passing onto and through the Project site is the integrated product of all of the runoff-producing storms that occur in the watershed, and all of these storms contribute to the stability and dynamics of the on-site washes and the quantity of sediment that is available to support sensitive habitat. Because it is not possible to determine specific storm events that meet these requirements, Tetra Tech used results from the hydrology analysis of the various storm hydrographs described in the Infiltration Report (Tetra Tech, 2011), additional hydraulic analysis of existing washes, and appropriate sediment transport relationships to estimate the quantity of sand carried onto and through the site on an individual storm basis and on an average annual basis under both existing and proposed project conditions. The resulting quantities of sediment were then compared to assess the effect of the Project on sediment loads within the site, and the likely response of the existing washes to any identified changes, including potential for changes in the both the short- and long-term stability and dynamics of the existing washes that could affect the safety of on- and off-site infrastructure and the amount of fine sand that is available for Aeolian entrainment from the washes and deposition on the dunes that comprise MTFH habitat.

This report describes the analysis that was performed to address the above conditions.

1.2 Authorization and Project Team

Tetra Tech, Inc. was retained by Calico to complete this analysis using site plans developed by Westwood Professional Services and other available information. Tetra Tech's Project Manager for this work was Dr. Robert Mussetter, PE, and he was assisted by Ms. Alaina Smith, and other Tetra Tech support staff.

During the early phases of Tetra Tech's work on the project, Dr. Mussetter participated in a field visit with representatives from Calico and Westwood. Representatives from the Commission also participated in a portion of the field visit. During the field visit, significant portions of the site were viewed by traversing the available access roads and walking portions of the site not directly accessible by vehicle. Eight grab samples of the bed-material sediments found within significant on-site washes were collected for laboratory sieve analysis to supplement the other available soils and sediment data.

2 GEOMORPHIC SETTING AND SEDIMENT-TRANSPORT PROCESSES

The watershed draining to and across the project site can be broadly divided into five zones (**Figure 2.1**):

1. the steep slopes and alluvial valleys of the Cady Mountains located to the north (**Figures 2.2 and 2.3**),
2. the coalesced alluvial fan (i.e., bajada) surface located downstream from the mountain front (Figure 2.3),
3. the relatively flat surface draining from the lava fields associated with the Pisgah Crater located to the south of Interstate 40 (I-40), and
4. the valley floor that generally lies between I-40 and the BNSF Railroad line (**Figure 2.4**).

The Cady Mountains comprise approximately 22 square miles, or about 36 percent, of the total 60-square-mile drainage basin. This portion of the watershed is characterized by steep (30 to 60 percent), bedrock slopes above alluvium-filled canyon bottoms that drain generally in a south-southwesterly direction onto the alluvial fan/bajada surface on which the Project site is located (Figures 2.2 and 2.3). The bajada surface is characterized by numerous shallow flow paths that also drain in a south-southwesterly direction at gradients ranging from 10 to 15 percent near the mountain front, to less than 5 percent at the distal end, near the BNSF Railroad line. The portion of the watershed located south of I-40 covers an area of approximately 13 square miles (about 22 percent of the total contributing watershed area), and generally drains in a west-northwesterly direction at slopes in the range of 5 percent. The valley bottom that generally lies between I-40 and the BNSF Railroad line drains to the west at slopes in the range of 5 percent or less.

2.1 Climate and Precipitation

2.1.1 General

Precipitation patterns in the Mojave Desert, in general, and specifically in the vicinity of the Project site, are strongly influenced by a rain-shadow effect caused by the surrounding mountainous terrain that significantly reduces winter season rainfall compared to coastal and mountain areas to the south and west. The area has a typical desert climate characterized by low precipitation, hot summers, mild winters, low humidity, and strong temperature inversions. Total rainfall at the nearest long-term precipitation gage, which is located Daggett Air Force Base, California, approximately 30 miles west of the Project site, averages about 3.9 inches per year, with about 70 percent of the total annual rainfall occurring during the winter rainy season (October through April), 25 percent to 30 percent occurring during late summer and early fall thunderstorms (July through September), and less than 5 percent occurring during the hot summer months (May and June) (Western Regional Climate Center [WRCC] 2010) (**Figure 2.5**).

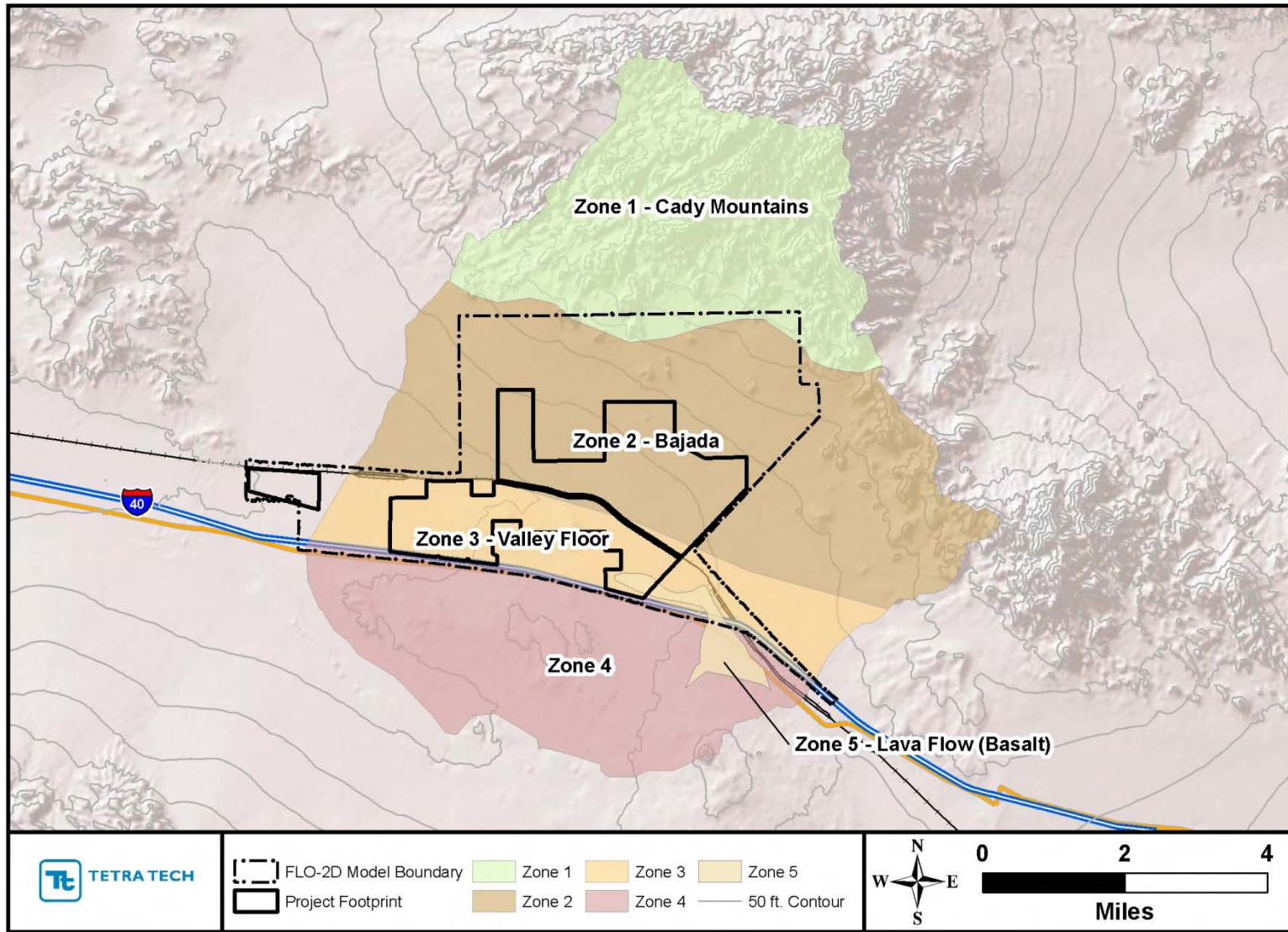


Figure 2.1. Topographic surface of the Project site and upstream watershed.

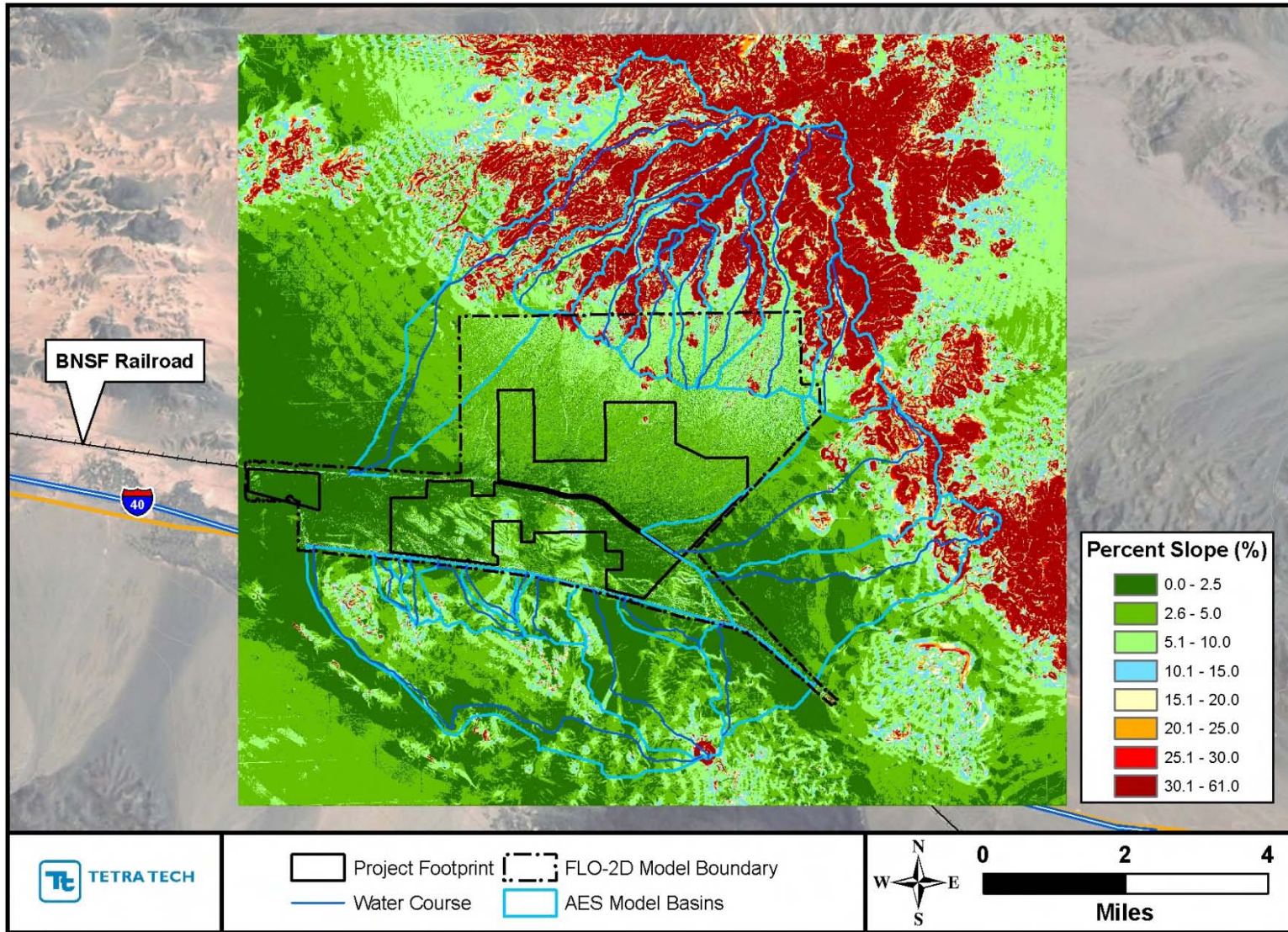


Figure 2.2. Topographic slopes at the Project site and upstream watersheds.



Figure 2.3. Typical view of the bajada surface covered by the Mojave creosote bush scrub vegetation community and Cady Mountains from southeast corner of Section 4 near the extension of Hector Road.



Figure 2.4. View looking downstream in the wash below BNSF Railroad Drainage Structure No. 4, near the center of Section 4 (see Figure 2.2 for location). Much of the fine sand that is visible in this photograph is a veneer of Aeolian origin over the coarser underlying alluvial sand.

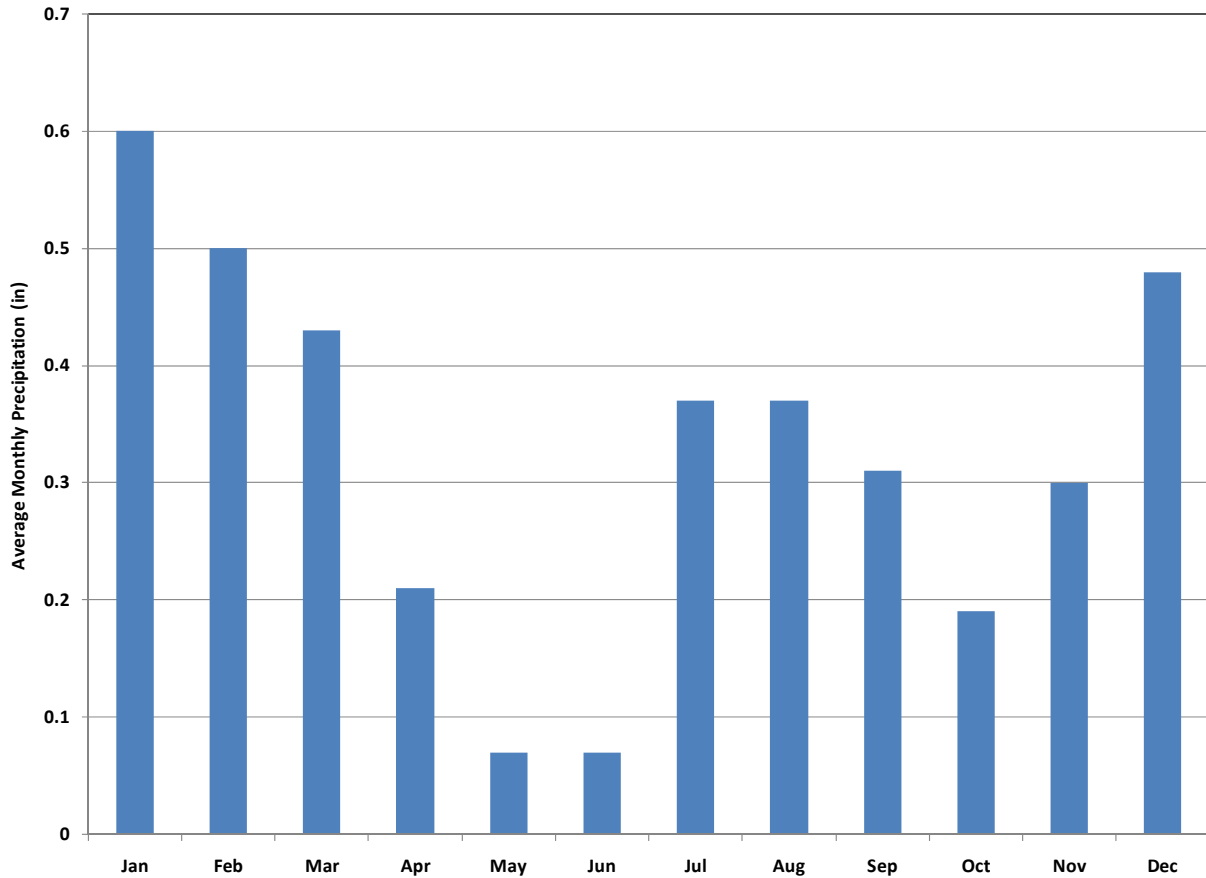


Figure 2.5. Average monthly precipitation from 1948 through 2010 at Daggett FAA Airport.

Although the most extensive and widespread rainfall occurs during the winter rainy season, the most dramatic events that produce sufficient runoff to transport significant quantities of sediment results from convective thunderstorms that occur during the late summer and early fall monsoon season in response to tropical cyclones and hurricanes that drift across the region from off the coast of Baja CA (Hereford et al., 2004). As described in the Infiltration Report, precipitation data available from the National Oceanic and Atmospheric Administration (NOAA) Atlas 14, Volume 6, Version 2 (April 2011) (<http://hdsc.nws.noaa.gov/hdsc/pfds/>) indicates that the 6- and 24-hour total point precipitation depths range from approximately 0.7 inches to 1.0 inches for a 2-year storm to 2.0 to 3.0 inches for the 100-year storm (**Table 2.1**). As described in the Infiltration Report (Tetra Tech, 2011) and summarized in the following section, results from the FLO-2D model of the Project site indicate that very little runoff occurs for the 2-year event, and the about 0.7 inches of the total 3 inches during the 24-hour storm is seen as surface runoff. As a result, sufficient runoff to fluvially entrainment significant quantities of sediment within and across the site occurs only on an episodic basis in about 1 of every 5 years, on average. Based on stratigraphic sections of the reservoir deposits in 14 “artificial reservoirs” created by railroad embankments spread through a portion of the Mojave Desert in eastern California and southern Nevada, Griffiths et al. (2006) found that the average recurrence interval of streamflow into the reservoirs was about 4.7 years and varied from 2.6 to 7.3 years over the period dating back to the early 1900s, and the average recurrence interval increased from 4.6 years prior to 1952 to 6.4 years during the period since 1952. The modeling results reported in the Infiltration Report are very consistent with these data.

Table 2.1. Approximate point precipitation depths (inches) for the watershed at the Project site.						
Duration	Recurrence Interval (years)					
	2	5	10	25	50	100
5-minute	0.13	0.18	0.23	0.30	0.36	0.42
30-minute	0.30	0.44	0.56	0.72	0.86	1.01
60-minute	0.41	0.59	0.74	0.97	1.15	1.35
3-hour	0.58	0.80	0.98	1.25	1.47	1.70
6-hour	0.70	0.96	1.17	1.48	1.73	1.99
24-hour	1.04	1.44	1.77	2.24	2.61	2.99

2.1.2 Effects of El Niño and La Niña

Episodes of unusually wet and dry climate occur in the Mojave Desert region that are linked with conditions in the tropical and northern Pacific Oceans. These episodes are caused by interrelated global-scale fluctuations of sea-surface temperature (SST), atmospheric pressure, and atmospheric circulation patterns (Cayan et al., 1999; Hereford et al., 2004). The fluctuations operate on two time scales: (1) short-term climate variation that has a typical period of 4 to 7 years, associated with El Niño and La Niña activity that is identified by several indicators, including the Southern Oscillation Index (SOI), equatorial SST, and more recently the Oceanic Niño Index (ONI) (**Figure 2.6**), and (2) longer-term variation that occurs over multi-decadal periods and follows a pattern best expressed by the Pacific Decadal Oscillation (PDO) in the North Pacific Ocean (Mantua and Hare, 2002; NOAA Climate Prediction Center, 2011). While there is considerable scatter in the data in Figure 2.6, there is a strong and statistically significant trend of increasing winter wet season precipitation and ONI. El Niño conditions are associated with warm SST in the tropical, eastern Pacific Ocean, and they tend to bring wet winters to the Southwestern U.S. through displacement of the storm tracks in a southerly direction. In contrast, La Niña conditions are associated with cooler SST and they bring reliably dry winters to the area (Hereford et al., 2004). The longer-term variations are associated with measurable shifts in the climate over periods of two to three decades. Warm phases of this oscillation occurred during the early part of the 20th century prior to the mid-1940s and the later part of the century from about 1977 through 1998, and a cool phase occurred between the mid-1940s and 1977. During the warm phases, annual precipitation tends to be higher than the long-term average, and during the cool phases, the annual precipitation tends to be lower.

The precipitation data on which the hydrology analysis was based represents average conditions over periods that span both the short- and long-term PDO cycles. Although systematic differences in precipitation occur between the warm and cool, long-term cycles, the shorter duration El Niño and La Niña cycles appear to have a more significant effect on the types of storms that deliver sediment to and across the Project site, with the attendant effects on channel dynamics and the availability of fine sand to support critical habitat. In general, the winter wet period from October through March during El Niño years tends to be wetter than usual across the southwestern U.S., including Mojave Desert Region, with more rainy days and more rain per rainy day (**Figure 2.7**). El Niño winters can be two to three times wetter than La Niña winters in this region. Eastern Pacific autumn tropical storms (i.e., late-summer and early-fall monsoonal storms) appear to be less frequent in El Niño years; however, the tropical storms that do occur have a greater than usual tendency to re-curve into Mexico or the southwest U.S., and the associated higher than usual water temperatures off the Mexican coast during El Niño

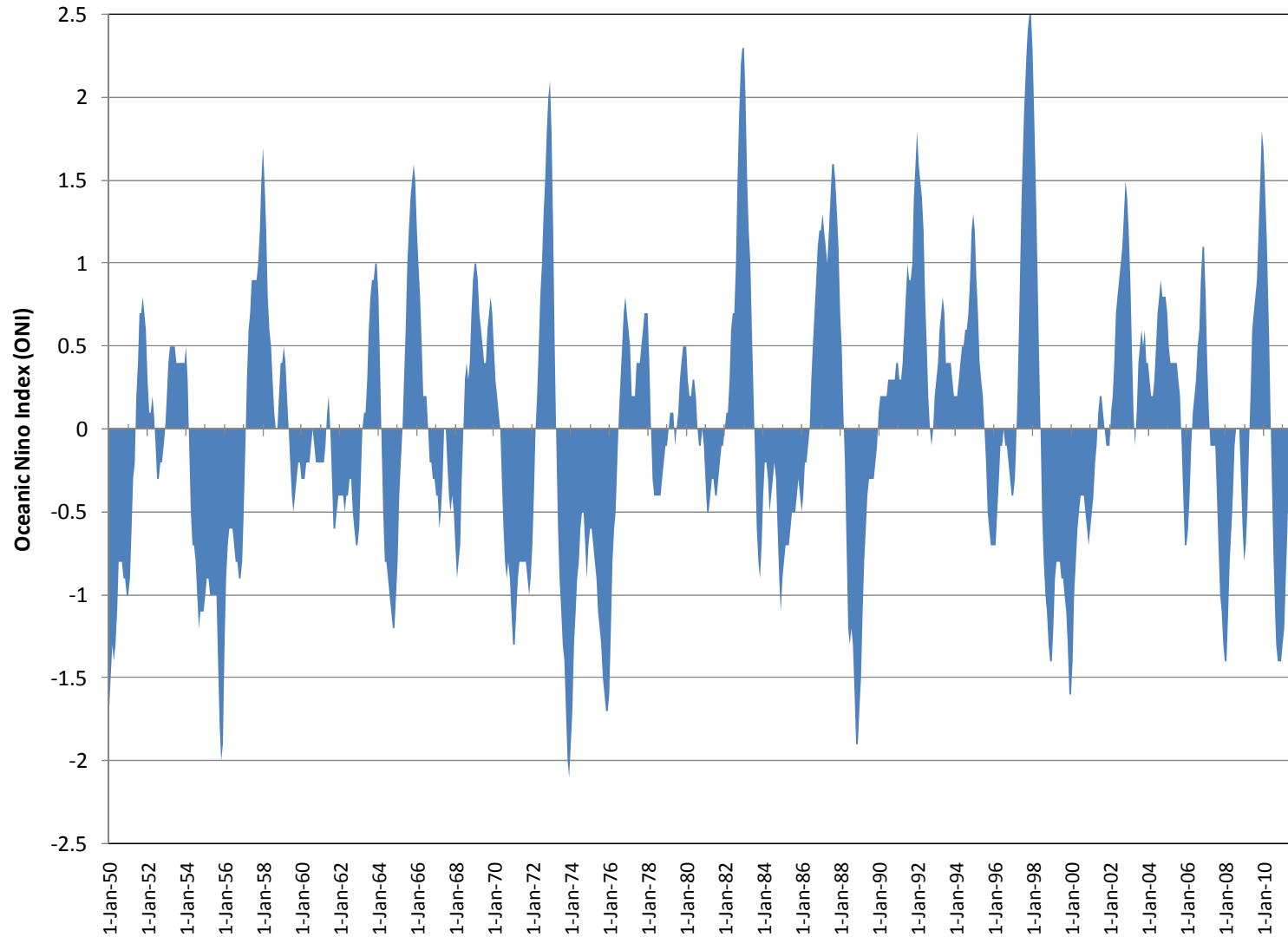


Figure 2.6. Oceanic Niño Index (ONI) for period from 1950 through mid-2011. Warm period corresponding to El Niño and La Niña conditions are defined as 5 consecutive overlapping tri-monthly periods exceeding ± 0.5 , respectively (i.e., El Niño > 0.5 , La Niña < 0.5) (from NOAA, 2011).

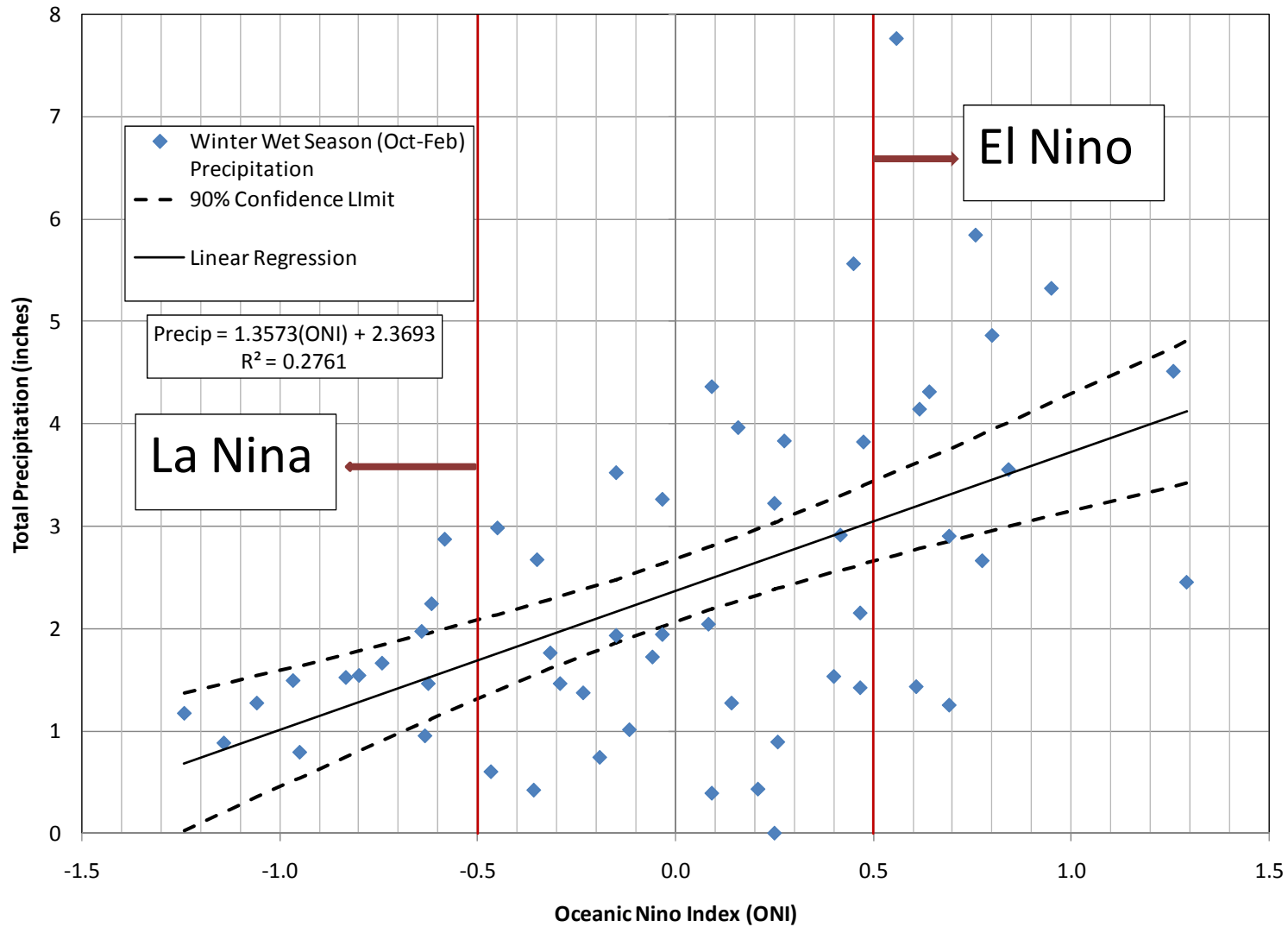


Figure 2.7. Relationship between total winter wet season (October through March) precipitation and Oceanic Niño Index (ONI) based on data from Daggett FAA Airport station.

years can cause these storms to be stronger than normal. In contrast, runoff producing events that result in significant sediment movement onto and across the site occur less frequently and are generally of smaller magnitude during La Niña years.

2.2 Soil, Vegetation, and Erodibility Factors

Due to its low potential for agricultural use, current soil-survey data are limited in much of the Mojave Desert, including the Project site. Nevertheless, mapping of hydrologic soil groups at a somewhat coarser scale is available from the NRCS STATSGO2 website, which can be found on-line at: <http://soils.usda.gov/survey/geography/statsgo> (Figure 2.8 and Table 2.2).

The surface soils in the watershed generally consist of Quaternary alluvium and fanglomerate composed of sediments washed down from the Cady Mountains located to the northeast of the Project site (BLM, 2010). Small outcrops of Tertiary basalt, andesite, and volcanic breccia occur in the northernmost portion of the Project site, and a small outcrop of “basalt flow” from the geologically recent Pisgah Crater eruption is present along the southernmost Project site boundary, but this does not appear to contribute runoff to the site and also prevents runoff from watersheds located farther to the south and east from entering the site (Figure 2.9).

Based on field observations, the available geologic mapping and other available information, the steep mountain slopes have significant bedrock outcrop that would limit infiltration rates and increase overall runoff, but would also limit sediment yields from the upper part of the basin (Figure 2.10). The alluvial fan/bajada surface lying north of the BNSF Railroad line, and at least a portion of the valley floor south of the BNSF line, is recently (geologically) deposited, relatively coarse-grained (sand and gravel) alluvium. Based on the five surface sediment samples collected by Tetra Tech from the bed of existing washes along the northern portion of the Project site during the 2011 field reconnaissance (Figure 2.11a, Samples S1 through S4 and S6), and the alluvium on the fan/bajada surface consists of about 60 percent sand, 40 percent gravel and a small amount (generally less than 2 percent to 3 percent) silt and clay (Figure 2.11b). The median (D_{50}) size of the representative gradation developed by averaging these five samples is approximately 0.87 mm (i.e., medium sand), and the D_{84} and D_{16} (sizes for which 84 and 16 percent of the material is finer) is 7.5 mm (fine gravel) and 0.23 mm (fine sand), respectively. The surface material in the wash shown in Figure 2.12 is typical of the material in the samples used to develop the representative gradation. The gradation of three samples collected by URS (2009) at depths in the range of four feet were similar to those from the Tetra Tech (2011) samples (Figure 2.13) providing additional confidence that these samples are representative of the bajada/fan surface. Sample S5 that was collected from the wash upstream from BNSF Drainage Structure No 4 (but outside the railroad right of way) was somewhat finer, with median size of 0.42 mm, likely due to the lower channel gradient and resulting lower flow energy in this area. The two samples collected in the washes downstream from BNSF Drainage Structures No 4 and 6 (but outside the right of way) (Samples S7 and S8) also have somewhat finer gradations (median sizes of 0.57 and 0.55 mm, respectively) due to the flatter slope and lower hydraulic energy.

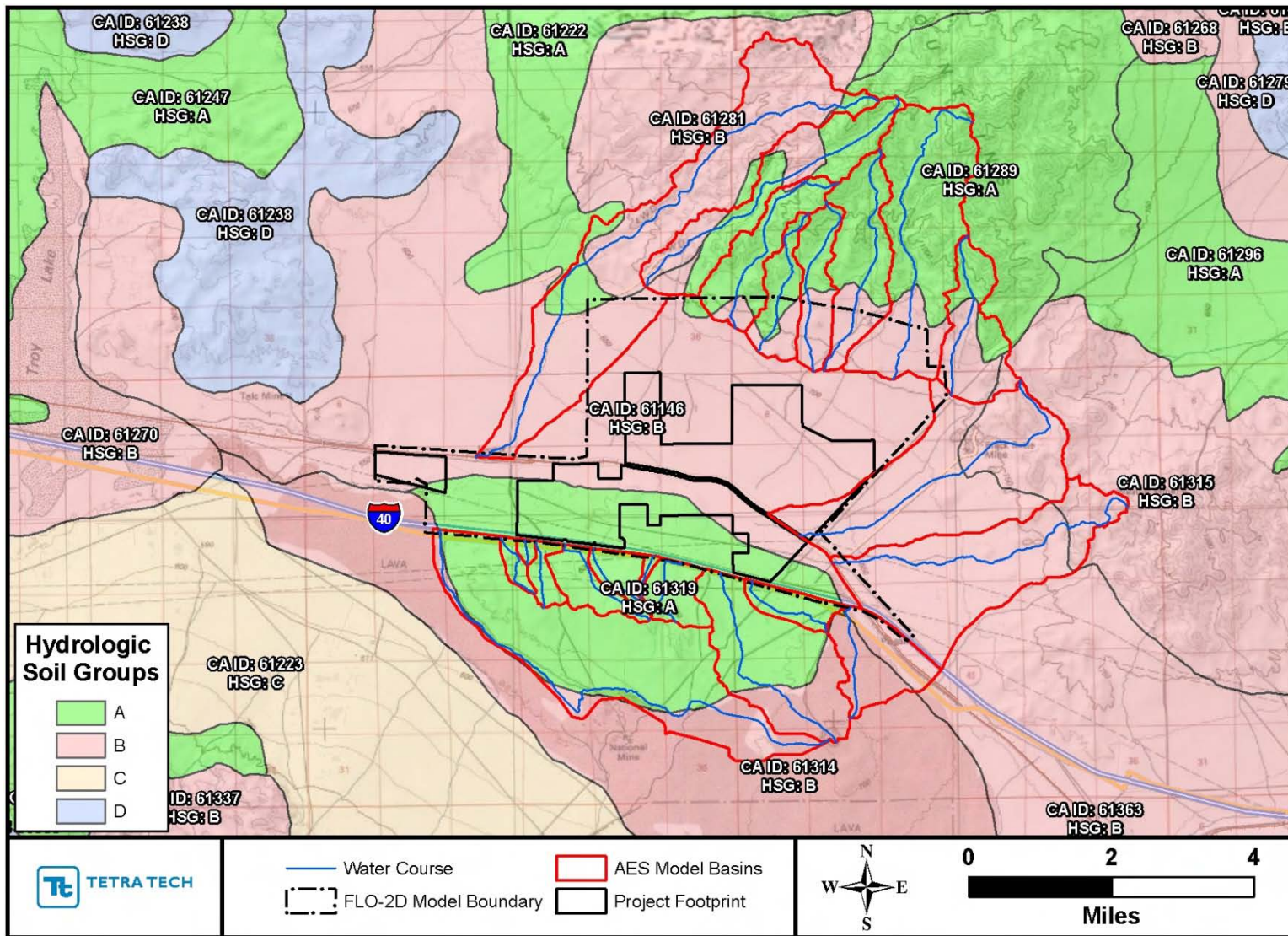


Figure 2.8. Hydrologic soil groups in the vicinity of the project from NRCS STATSGO2 website.

Table 2.2. Description of soils in the project watersheds from NRCS STATSGO2 mapping (see Figure 3).

CA Identification Number	Composite Soil Name	Mapping Unit Name	Texture	Slope Range (%)	Premeability (in/hr)	Shrink-swell Potential	Hydrologic Soil Group	Soil Erodibility Factor (K)	Percent Silt/Clay
61146	CHUCKAWALLA	CARRIZO-ROSITAS-GUNSIGHT	Gravelly silty loam	0-30	2-6	LOW	B	0.24	15
61281	LAVIC	ROCK OUTCROP-UPSPRING-SPARKHULE	Loamy fine sand	0-5	20	LOW	B	0.2	15
61289	CAJON	ROCK OUTCROP-LITHIC TORRIORTHENTS-CALVISTA	Sand	0-8	0.2-0.6	MODERATE	A	0.1	30
61315	LAVIC	ROCK OUTCROP-UPSPRING-SPARKHULE	Loamy fine sand	0-5	20	LOW	B	0.2	30
61319	ARIZO	NICKEL-ARIZO-BITTER	Gravelly loamy sand	2-8	2-6	LOW	A	0.1	15

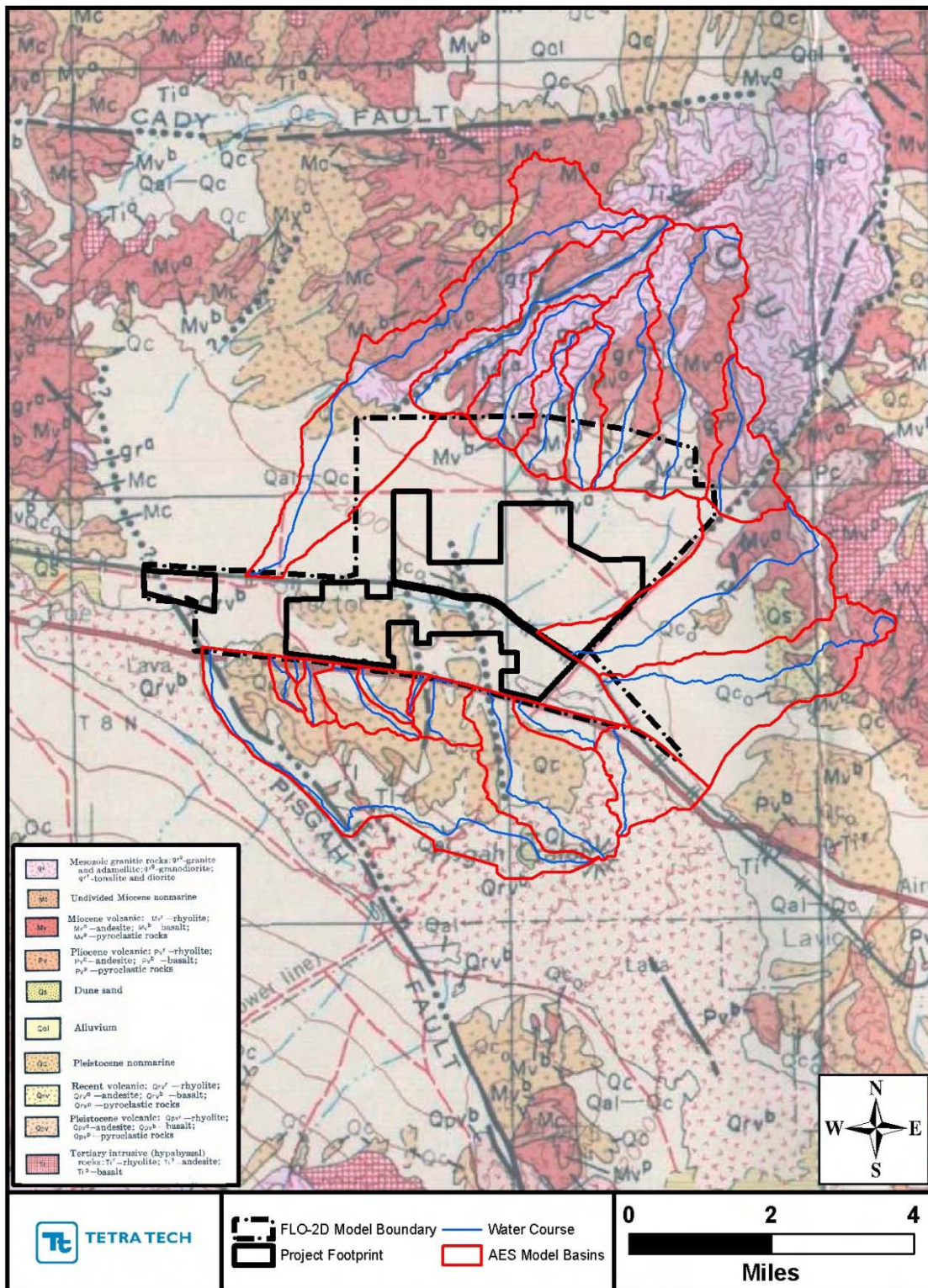


Figure 2.9. Geology map of the vicinity of the Project site.

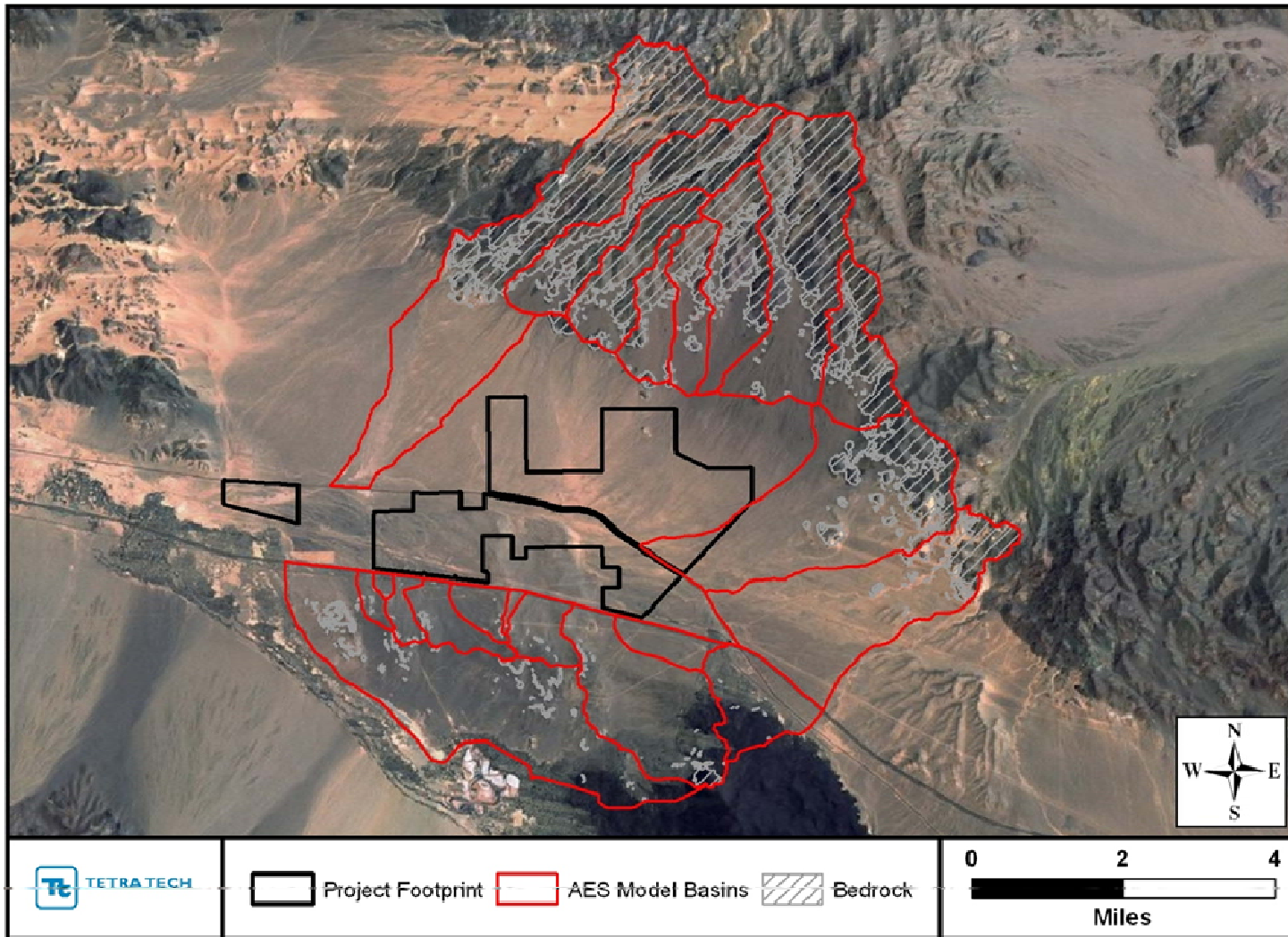


Figure 2.10. Aerial photograph (June 14, 2009) of watershed showing the bedrock and alluvial surfaces.

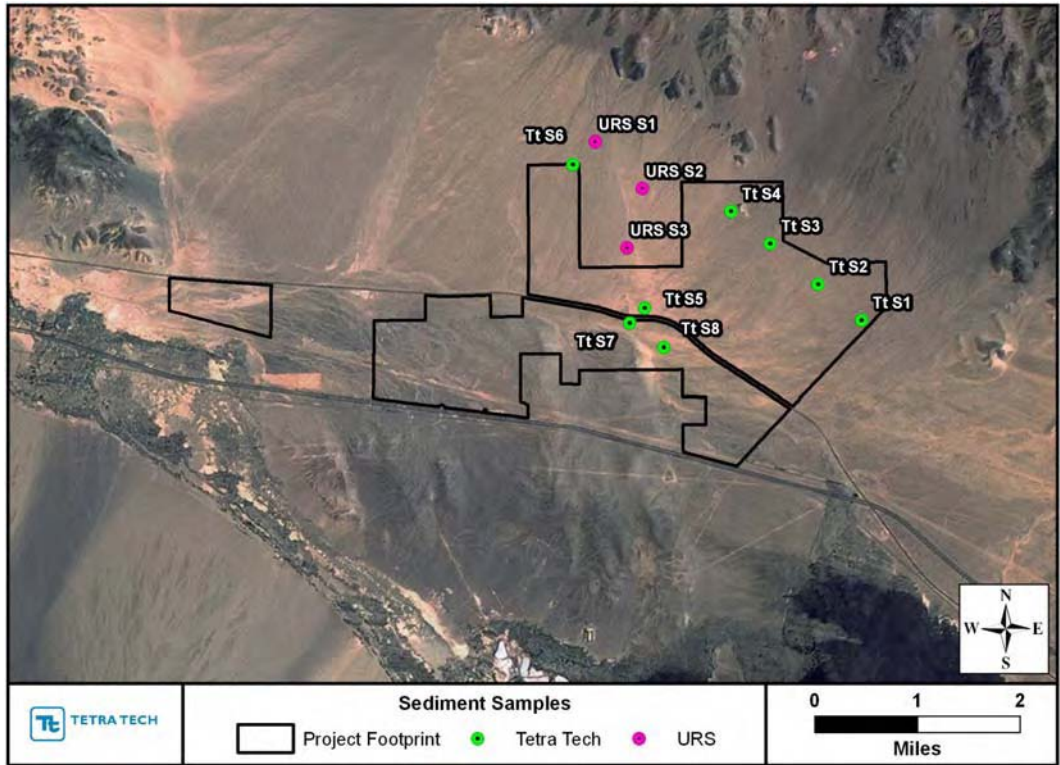


Figure 2.11a. Location of surface sediment samples collected by Tetra Tech (2011) and URS (2009).

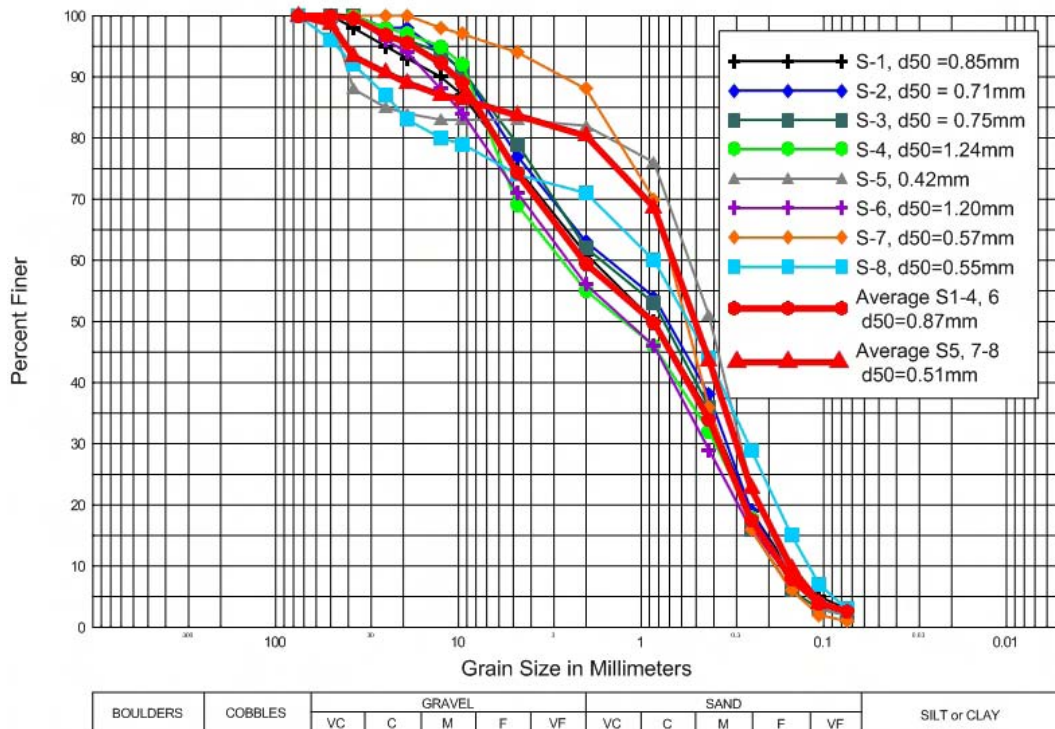


Figure 2.11b. Particle size distribution curves for samples collected by Tetra Tech (2011).



Figure 2.12. View looking downstream in a well-defined wash along north boundary of the Project site near Sample S4 showing the typical surface bed-material characteristics.

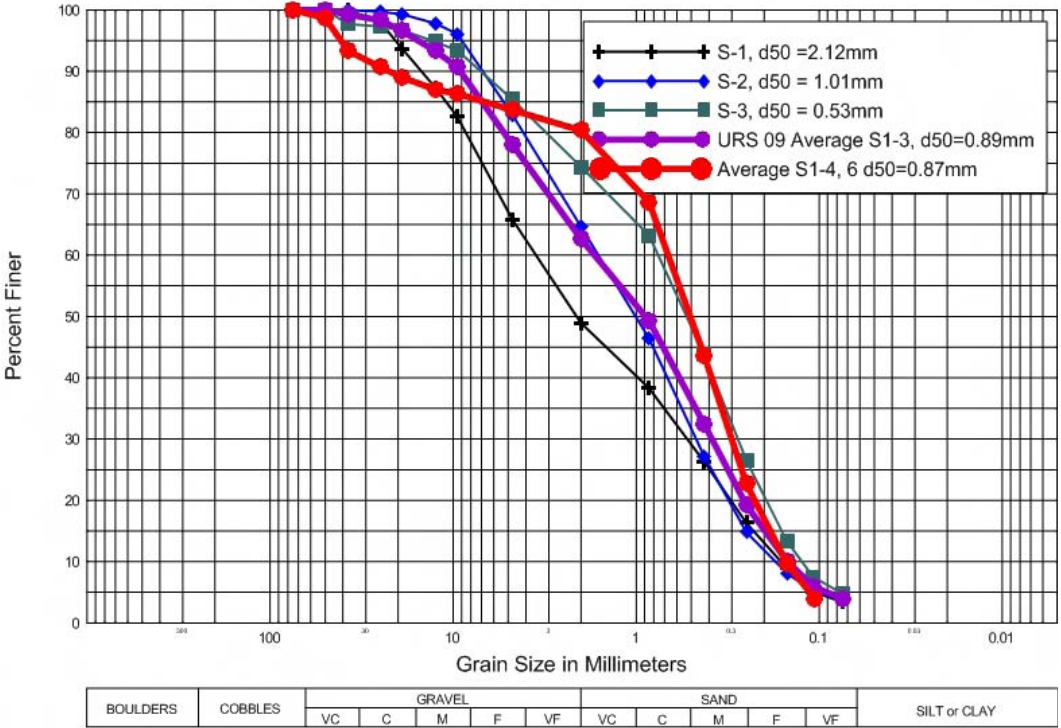


Figure 2.13. Particle size distribution curves for three near-surface sediment samples collected by URS (2009).

In addition to the soil characteristics, vegetation also plays an important role in determining the runoff and sediment yield characteristics of the watershed. As described in BLM (2010), the Biological Resources Technical Report for the previously submitted “Solar One Project” (SES 2009) identified two vegetation communities on the site: (1) Mojave creosote bush scrub, and (2) desert saltbush scrub. Of these two communities, the Mojave creosote bush scrub occupies over 97 percent of the site (**Figure 2.14**). The community description used for the vegetation mapping follows the relatively coarse-scale classification system described by Holland (1986) that combines several vegetation associations that occupy specific portions of the site into the broader Mojave creosote bush scrub classification. While they have not been mapped, the smaller vegetation associations include microphyll woodlands such as catclaw acacia thorn scrub that are typically associated with dry desert washes; lower elevation wash and sand-field vegetation; smoke tree woodland; and big galleta shrub-steppe.

The characteristics of this community that affect rainfall-runoff and sediment yield processes include the widely spaced distribution of the shrubs that occur, along with a diverse assemblage of annual and perennial herbs that establish during periods of adequate seasonal precipitation. A number of cactus species also occur on the Project site. In general, this community corresponds to the Desert Brush category, with 20-percent cover in SBC (1986, Figure C-8) for purposes of defining the runoff CNs and associated rainfall interception characteristics.



Figure 2.14. View looking NE across the bajada/fan surface toward to Cady Mountains showing the typical Mojave creosote bush scrub community.

3 SITE HYDROLOGY AND HYDRAULIC ANALYSIS

As described in the Infiltration Report (Tetra Tech, 2011), runoff from the majority of the off-site basins during storms from the 2- through 100-year, 6- and 24-hour duration, events were estimated using procedures specified in the San Bernardino County (SBC) Hydrology Manual (SBC, 1986; 2010), as implemented in the Advanced Engineering Software (AES) Flood Routing Analysis Computer Program, 2009 version (Figure 1.1, **Tables 3.1 and 3.2**). The resulting flow hydrographs were then combined with runoff resulting from on-site precipitation and routed across the Project site using the FLO-2D model (FLO-2D Software, 2009) to determine the flow hydrographs and associated hydraulic and sediment-transport conditions throughout the site. Because the AES model provides estimates of the flow at individual nodes, the downstream boundary of the subbasins used in the AES model were located well upstream from the Project site boundary near the apex of the alluvial fans, and the FLO-2D model grid includes the area between the downstream basin nodes in the AES model and the Project site boundary to insure that the flow from the AES hydrographs is allowed to spread onto the alluvial fan surface before reaching the site (**Figure 3.1**).

3.1 Existing Conditions Model

The FLO-2D model for the Project is comprised of approximately 218,700 nodes, with each node representing a square grid, 50 by 50 feet, covering a total surface area of about 20 square miles. The elevations for each grid were assigned in FLO-2D based on the average elevation of the 2,500-square-foot area of each node, as determined from the LiDAR mapping. A Manning's roughness coefficient of 0.04 was used in the model for overland flow where vegetation and surface irregularities affect the roughness (Figure 2.12), and a Manning's roughness coefficient of 0.035 was used for the well-defined, mostly unvegetated channels (Figure 2.10). The available aerial photography was used to identify channels of sufficient width that were mostly devoid of vegetation for application of the lower roughness coefficient.

The BNSF Railroad is identified in the model as a levee that is allowed to overtop without failure. This provides a mechanism for evaluating the potential for overtopping of the railroad, and the maximum depth and duration of overtopping where it occurs under both existing and project conditions. The trestles and box culverts that provide drainage pathways through the railroad grade (Figure 3.1) are incorporated into the model by providing openings in the levee with have restricted width and increased Manning's roughness coefficients that produce water-surface elevation versus discharge rating curves that are consistent with curves from local one-dimensional (1-D) models that were developed using the Hydraulic Engineering Center - River Analysis System (HEC-RAS) software. The detailed procedures for developing the rating curves are described in the Infiltration Report (Tetra Tech, 2011).

Flows generated from rainfall directly on the Project site are simulated in the FLO-2D model using procedures that are consistent with the San Bernardino County procedures employed in the AES model for the off-site basins. Similar to the approach used in the AES model, the runoff curve numbers (CN) in the FLO-2D model vary with both storm depth and duration (**Table 3.3**).

3.2 Proposed Conditions Model

The proposed conditions model was adjusted to represent the features that will be added by the Project, including roads, buildings, parking areas, PV arrays, and SunCatchers™ (**Figure 3.2**).

Table 3.1. Peak discharges (cfs) at the FLO-2D inflow nodes for the 2-, 5-, 10-, 25-, 50- and 100-year storms under existing conditions.

Basin ID	Area (mi ²)	6-hour Storm						24-hour Storm					
		2-year	5-year	10-year	25-year	50-year	100-year	2-year	5-year	10-year	25-year	50-year	100-year
10	6.85	38	273	684	1,294	1,791	2,354	37	264	659	1,256	1,782	2,335
11	2.51	21	154	366	878	1,154	1,430	20	146	354	852	1,119	1,413
12	1.43	15	109	258	697	910	1,132	15	105	250	679	891	1,109
13	0.92	12	86	198	520	666	832	11	81	190	503	649	812
14	1.03	13	92	214	510	657	819	12	87	204	492	640	805
15	1.91	19	132	311	802	1,060	1,307	17	125	299	775	1,027	1,287
16	4.11	28	204	497	1,367	1,815	2,273	27	196	480	1,333	1,763	2,239
17	1.54	17	116	273	827	1,056	1,318	15	110	261	798	1,033	1,295
18	5.19	39	242	598	1,399	1,934	2,534	31	225	555	1,319	1,884	2,467
19	4.29	31	219	534	1,288	1,767	2,305	28	201	493	1,209	1,716	2,233
20	1.36	15	109	254	598	802	1,006	14	102	242	580	778	976
21	0.52	9	63	143	289	378	473	8	58	134	275	360	459
22	2.9	25	173	415	1,022	1,349	1,756	22	159	387	974	1,309	1,704
23	0.65	10	72	164	401	525	652	9	66	154	382	508	640
24	0.07	3	19	41	60	76	95	3	18	38	57	74	92
25	0.41	8	54	122	291	376	467	7	50	114	278	364	455
26	0.65	10	72	164	366	477	599	9	66	153	349	462	582
27	0.29	7	44	99	227	291	359	6	41	93	217	283	350
28	0.07	3	20	42	85	108	131	3	18	40	82	105	129
29	0.19	5	35	77	135	175	216	5	32	72	129	169	210
30	5.85	37	256	628	928	1,284	1,698	33	241	598	887	1,272	1,676

Table 3.2. Runoff volumes (ac-ft) at the FLO-2D inflow nodes for the 2-, 5-, 10-, 25-, 50- and 100-year storms under existing conditions.

Basin ID	Area (mi ²)	6-hour Storm						24-hour Storm					
		2-year	5-year	10-year	25-year	50-year	100-year	2-year	5-year	10-year	25-year	50-year	100-year
10	6.85	0.7	18.8	78.8	189.7	279.2	387.8	5.8	48.7	128.9	259.2	403.3	559.3
11	2.51	0.2	6.1	25.2	104.4	146.6	187.4	2.8	22.5	57.8	145.7	205.6	273.5
12	1.43	0.1	2.5	10.2	56.1	78.8	103.9	1.3	10.4	26.6	77.8	110.8	147.1
13	0.92	0.1	1.7	6.8	34.3	48.3	63.8	0.7	6.3	16.0	45.7	65.8	87.6
14	1.03	0.1	2.3	9.6	40.4	55.6	73.9	1.0	8.1	20.6	53.6	76.0	103.3
15	1.91	0.1	3.9	16.1	77.9	110.9	141.8	1.8	15.0	38.8	106.9	153.1	203.8
16	4.11	0.2	7.2	30.4	164.5	234.9	303.9	3.9	31.2	80.4	236.8	335.9	447.2
17	1.54	0.1	2.2	8.9	61.7	84.3	111.5	1.2	9.9	25.6	84.6	119.4	160.2
18	5.19	0.3	8.1	34.2	128.1	193.8	274.7	2.6	22.7	62.5	163.3	267.1	383.8
19	4.29	0.2	6.3	25.7	104.9	157.3	224.7	2.0	17.2	47.1	129.6	213.7	305.0
20	1.36	0.1	2.6	10.4	42.4	62.7	84.4	0.9	7.9	20.8	55.6	83.4	114.0
21	0.52	0.1	1.4	5.5	16.3	24.0	32.3	0.4	3.4	8.8	20.1	30.4	42.9
22	2.9	0.2	4.6	19.1	82.8	119.7	169.1	1.6	13.7	37.9	104.8	161.1	229.6
23	0.65	0.0	1.1	4.2	19.6	28.3	38.0	0.3	3.2	8.2	23.6	36.2	51.0
24	0.07	0.0	0.3	1.2	2.1	3.0	4.1	0.1	0.6	1.5	2.6	3.8	5.3
25	0.41	0.0	0.7	2.7	12.2	17.4	23.5	0.2	2.0	5.2	14.6	22.1	30.3
26	0.65	0.0	1.3	5.0	19.4	27.8	37.4	0.4	3.4	8.9	23.3	35.3	48.2
27	0.29	0.0	0.5	2.1	8.8	12.6	16.9	0.2	1.5	3.8	10.4	15.8	21.6
28	0.07	0.0	0.2	0.6	2.3	3.2	4.3	0.0	0.4	1.1	2.7	4.0	5.5
29	0.19	0.0	0.6	2.3	5.8	8.3	11.2	0.1	1.3	3.3	6.9	10.4	14.2
30	5.85	1.0	24.5	97.3	145.2	212.7	295.8	4.7	41.6	114.8	183.1	290.8	403.2

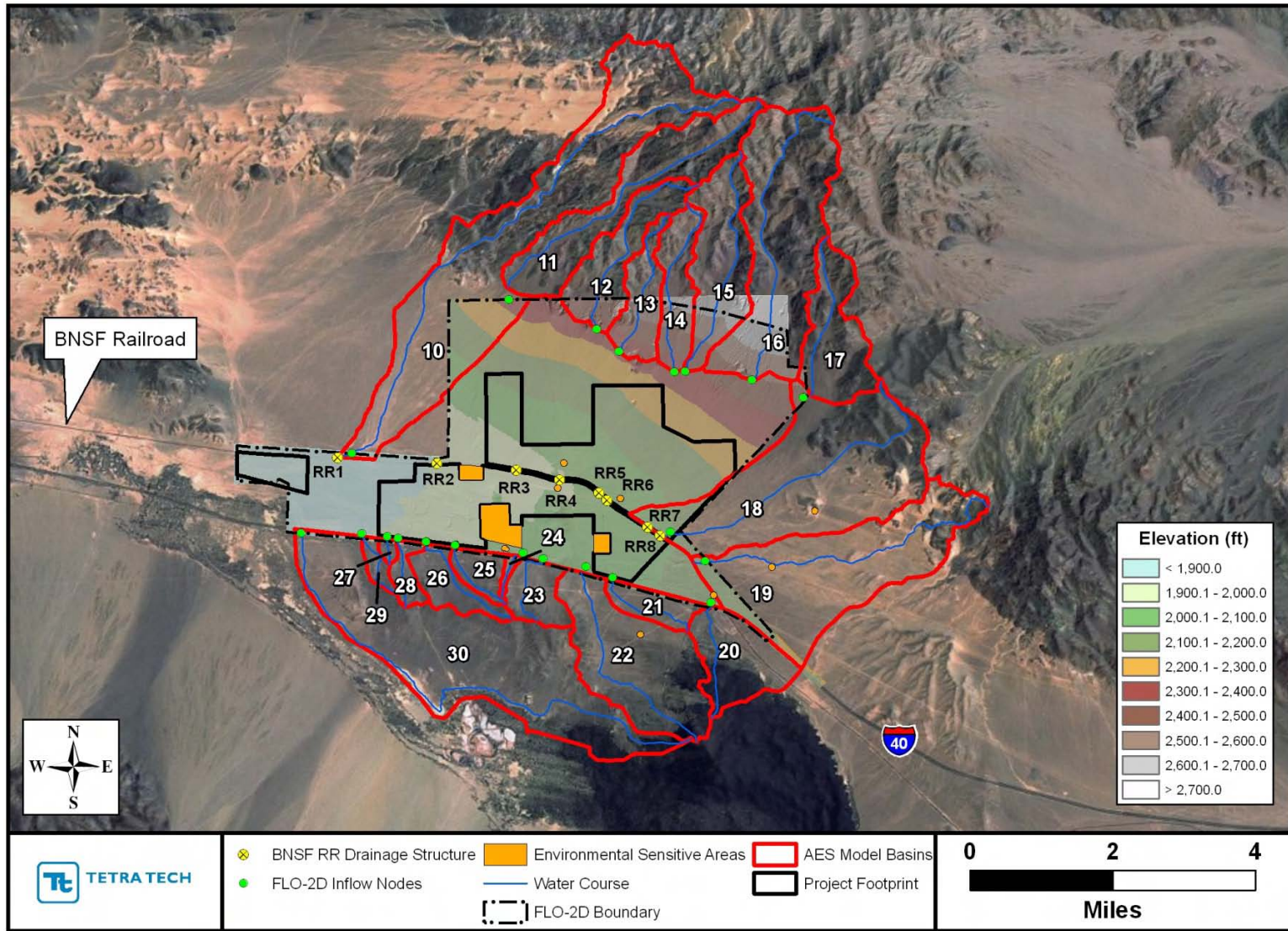


Figure 3.1. Map of Project site and contributing drainage subbasins showing the locations of the FLO-2D inflow nodes for the off-site basins and the BNSF railroad drainage structures.

Table 3.3. FLO-2D hydrologic parameters.								
Recurrence Interval (years)	6-hour Storm				24-hour Storm			
	Total Rainfall Depth (in.)	CN	Initial Abstration (in.)	Excess Runoff (in.)	Total Rainfall Depth (in.)	CN	Initial Abstration (in.)	Excess Runoff (in.)
2	0.69	68.2	0.69	0.00	1.01	62.8	1.01	0.00
5	0.93	68.2	0.93	0.00	1.39	62.8	1.18	0.01
10	1.14	68.2	0.93	0.01	1.71	62.8	1.18	0.04
25	1.44	69.8	0.87	0.07	2.16	64.7	1.09	0.18
50	1.68	73.1	0.74	0.19	2.52	68.5	0.92	0.41
100	1.93	75.6	0.65	0.37	2.89	71.4	0.80	0.72

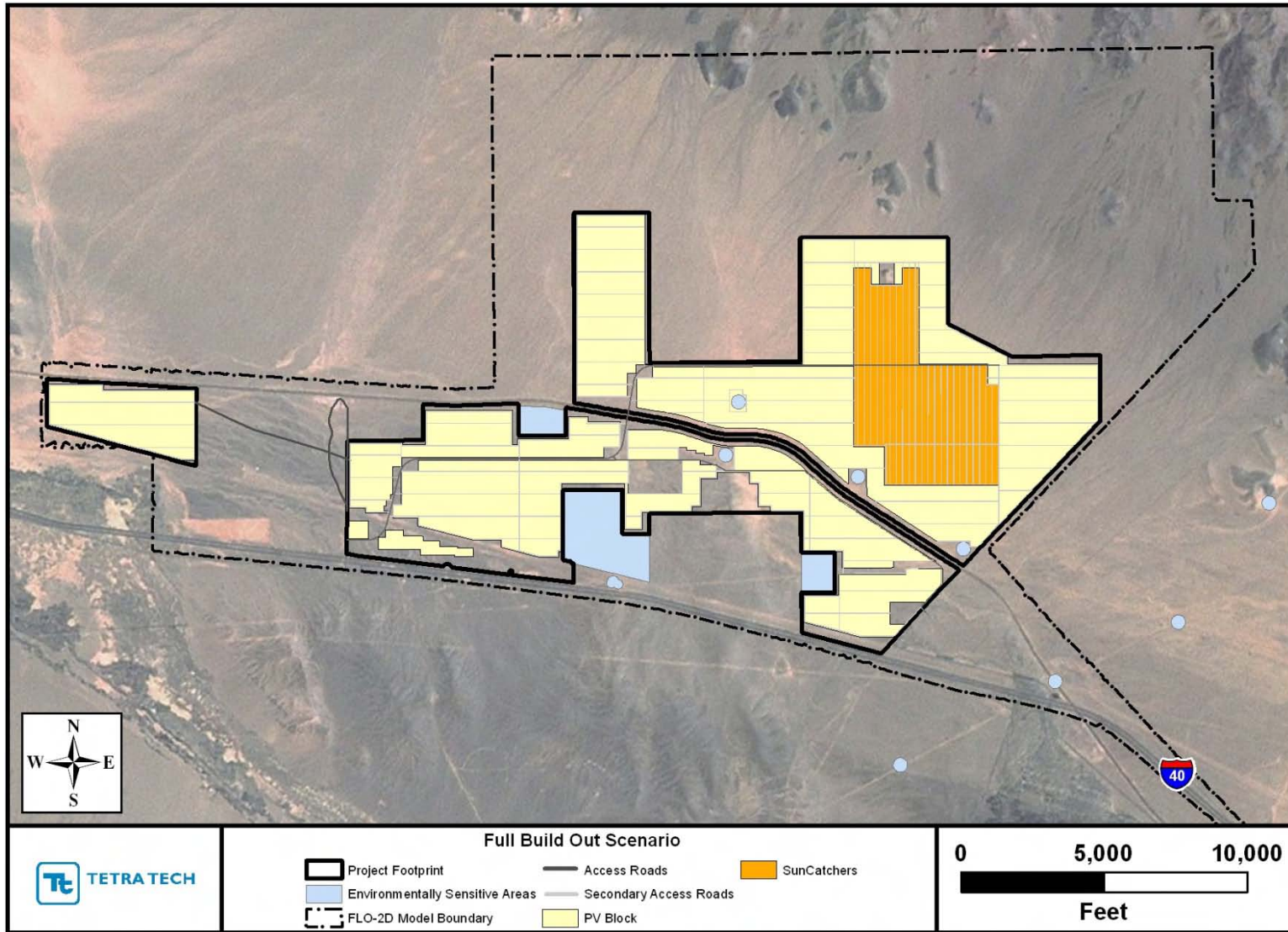


Figure 3.2. Project site map showing features under full build-out conditions.

The main service road will consist of an embankment that will be raised above the existing ground level and covered with a 24-foot-wide strip of 4-inch-thick asphaltic concrete. Culverts will be constructed in the main drainage paths to pass stormwater through the road. The secondary access roads will be constructed at existing grade, including a 6-inch-thick aggregate base course with soil stabilizer, to allow stormwater runoff to pass through the same drainage paths that are present under existing conditions. The main and secondary access roads were incorporated into the model by adjusting the affected grid elevations, as appropriate (main access road, only), increasing the CNs to account for the effects of compaction and surface paving on infiltration rates, and decreasing the Manning's roughness values to represent the decreased resistance to flow associated with the generally smoother surface. Manning's roughness coefficients of 0.025 and 0.033 were used for the main and secondary access roads, respectively.

The main service complex was represented in the model by adding area reduction factors (ARFs) at the proposed buildings to block flow and prevent water storage in the area occupied by the buildings, adjusting the CN to account for the effects of surface compaction and paving on infiltration and runoff response, and altering the Manning's roughness coefficient to account for the generally smoother surface in the parking lots and lay-down areas. The ARF values for the buildings were set to 1.0 where the building occupies essentially the entire grid, and to the appropriate percentage, where the building occupies only a portion of the grid. The parking lots and lay-down areas during construction were assumed to be impervious. For both locations, the Manning's roughness coefficient was reduced to 0.022 to represent the reduced resistance to flow.

The PV arrays are made up of tracker blocks which consist of a series of rows containing modules mounted on common shafts and controlled by a single tracker motor. This shaft is oriented north-south and is the axis around which the modules follow the sun as it travels east to west (**Figure 3.3**). The individual modules are approximately 3.4 feet wide by 6.5 feet long. Typical tracker blocks contain about 19 rows and are approximately 172 feet wide and 280 feet long. There is over 10-foot minimum of clear spacing between the rows with the modules in the horizontal position. The modules are supported above the ground by 4.5- and 6-inch diameter posts spaced at approximately 12- to 15-foot intervals along their length. With the minimum of approximately 10-foot open spacing between modules, at mid-day, the modules cover only 25 percent of the ground area. The percentage of the ground that is covered during other parts of the day decreases with other module orientations based on the relationship between the sun and the particular orientation of the array.

The SunCatchers™ consist of 38-foot diameter mirrored dishes that are supported above the ground by 2-foot diameter posts spaced at intervals of 112 feet in the east-west direction and 56 feet in the north-south direction (**Figure 3.4**). The SunCatchers™ will be constructed in a of the Project site on the north side of the BNSF Railroad, as shown in Figure 3.6. The SunCatchers™ rotate about on both a horizontal and vertical axis to optimize their angle with the sun. When oriented with their axis in the vertical direction, each dish covers an area of approximately 1,134 ft², or about 18 percent of the total ground area and about 45 percent of the 50- by 50-foot model grid cell in which they are located. The percentage of cover, of course, decreases with other orientations of the dish.

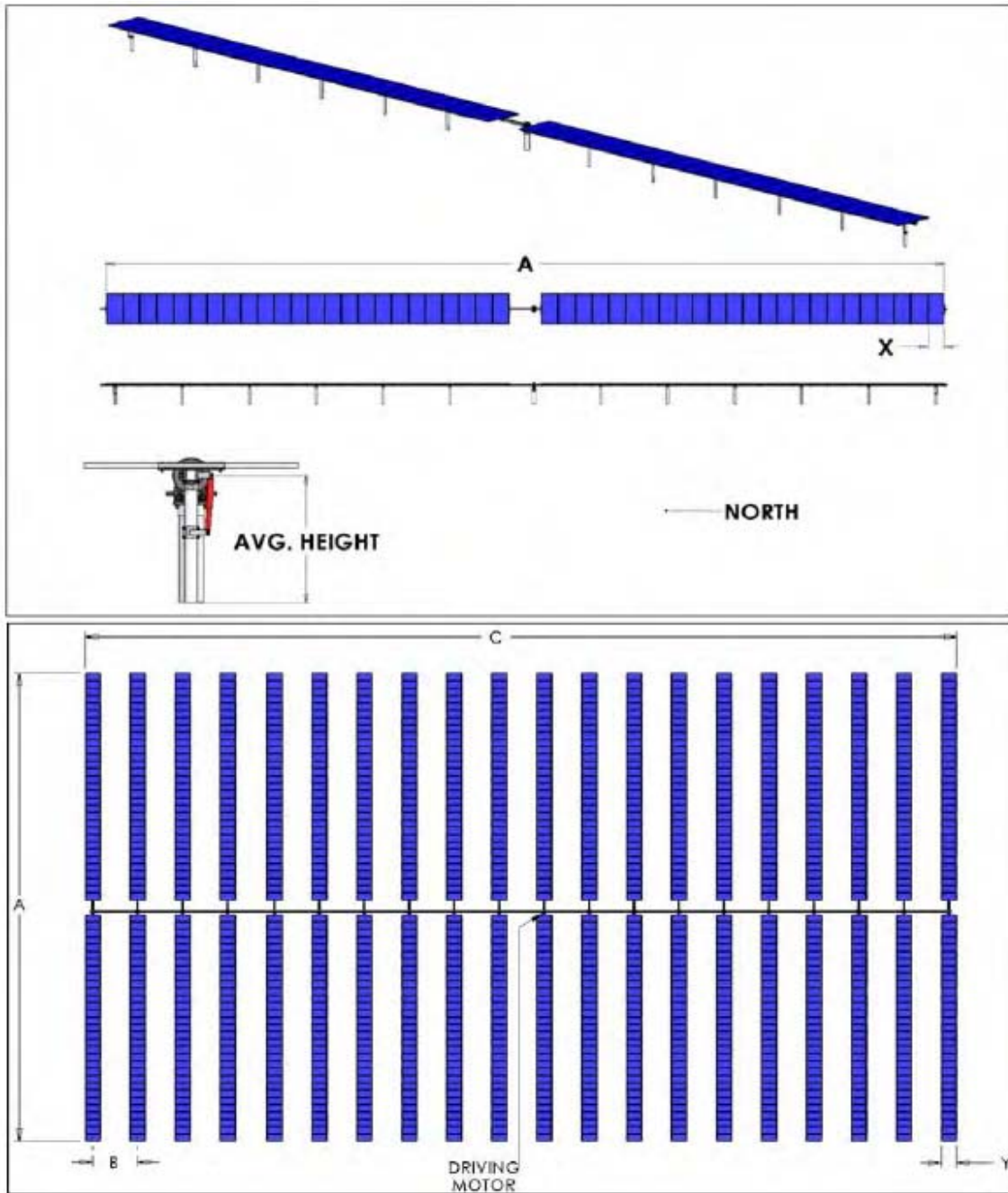


Figure 3.3. Typical PV panel layout (A=171 feet, B=19.6 feet, C=281 feet, X=3.4 feet, Y=6.5 feet).



Figure 3.4. Photo of typical SunCatchers™.

3.3 Model Results

3.3.1 Existing Conditions

For purposes of this geomorphology report, the model was executed for existing conditions (Figure 3.1) and full build-out conditions (Figure 3.2) for the 6- and 24-hour durations, 2-, 5-, 10-, 25-, 50- and 100-year recurrence interval events (total of 18 model runs). Results from the existing conditions rainfall-runoff models indicate that flows reaching the site from the offsite basins are relatively small, ranging from about 3 cfs (Basin 24) to less than 40 cfs (Basin 10) during the 2-year storm, and increasing to 90 to 100 cfs (Basin 24) to about 2,500 cfs (Basin 18) for the 100-year storm (Table 2.6). The existing conditions FLO-2D model results that account for the movement of these flows across the site, as well as the accumulation, infiltration and surface movement of rainfall directly on the site, indicate that flow volumes leaving the overall Project site range from about 0.3 ac-ft during the 2-year storm to about 3,900 ac-ft for the 100-year, 24-hour duration storm (**Tables 3.4 and 3.5**). These runoff amounts equate to less than 0.01 inches of runoff spread uniformly over the basin for the approximately 1-inch precipitation that occurs during the 2-year storm, and about 1.2 inches of runoff for the 100-year storm, compared to the total precipitation of approximately 2.9 inches. Tables 3.4 and 3.5 summarize key values from the FLO-2D model output for both the 6- and 24-hour duration storms, and **Figures 3.5a and 3.5b** show the distribution of maximum depths and velocities throughout the FLO-2D model grid for the 100-year, 24-hour storm under existing conditions.

Flows that reach the BNSF Railroad pass through the railroad at a series of drainage structures. Detailed evaluation of the model results indicates that some of these drainage structures, coupled with overflow channels on the north side of the railroad, have insufficient capacity to pass the entire flow reaching that particular location, in which case, the railroad line is overtopped (**Table 3.6**). Overtopping occurs in four locations during the 100-year recurrence

Table 3.4. FLO-2D results summary for the 6-hour storm event.

	2-Year		5-Year		10-Year		100-Year	
	Existing	Proposed*	Existing	Proposed*	Existing	Proposed*	Existing	Proposed*
Maximum Velocity (ft/s)	3.06	3.06	5.07	5.07	7.31	7.30	11.41	11.41
Average Velocity (ft/s)	0.01	0.01	0.10	0.10	0.20	0.20	0.69	0.70
Median Velocity (ft/s)	0.00	0.00	0.00	0.00	0.00	0.00	0.00	0.00
Maximum Depth (ft)	1.73	1.73	2.43	2.43	3.43	3.42	6.09	6.10
Average Depth (ft)	0.01	0.01	0.04	0.04	0.08	0.08	0.25	0.25
Median Depth	0.00	0.00	0.00	0.00	0.00	0.00	0.02	0.03
Inflow								
Rainfall (ac-ft)	720	720	970	970	1,189	1,189	2,013	2,013
Inflow Hydrograph (ac-ft)	27	27	214	214	552	552	2,591	2,591
Total Inflow (ac-ft)	747	747	1,185	1,185	1,741	1,741	4,604	4,604
Outflow								
Infiltration & Interception (ac-ft)	720	720	970	969	1,189	1,187	1,755	1,742
Floodplain Storage (ac-ft)	27	27	130	130	200	194	434	429
Outflow Hydrograph (ac-ft)	0.28	0.28	84	86	352	360	2,416	2,432
Total Outflow and Floodplain Storage (ac-ft)	747	747	1,185	1,185	1,741	1,741	4,604	4,604

*Proposed Condition represents the full build out (including all areas to the north of the railroad and to the west of the main service complex. Partial build-out conditions results are not present here because they generally fall between the existing and proposed result, which are very similar.

Table 3.5. FLO-2D results summary for the 24-hour storm event.

	2-Year		5-Year		10-Year		100-Year	
	Existing	Proposed*	Existing	Proposed*	Existing	Proposed*	Existing	Proposed*
Maximum Velocity (ft/s)	2.70	2.70	4.99	4.99	7.17	7.18	11.88	11.89
Average Velocity (ft)	0.01	0.01	0.10	0.11	0.21	0.21	0.82	0.83
Median Velocity (ft)	0.00	0.00	0.00	0.00	0.00	0.00	0.21	0.21
Maximum Depth (ft)	1.73	1.72	2.37	2.37	3.36	3.36	6.52	6.53
Average Depth (ft)	0.01	0.01	0.04	0.04	0.08	0.08	0.29	0.29
Median Depth (ft)	0.00	0.00	0.00	0.00	0.00	0.00	0.06	0.07
Inflow								
Rainfall (ac-ft)	1,054	1,054	1,450	1,450	1,784	1,784	3,015	3,015
Inflow Hydrograph (ac-ft)	32	32	271	271	719	719	3,546	3,546
Total Inflow (ac-ft)	1,086	1,086	1,721	1,721	2,503	2,503	6,560	6,560
Outflow								
Infiltration & Interception (ac-ft)	1,054	1,052	1,443	1,437	1,739	1,730	2,268	2,248
Floodplain Storage (ac-ft)	32	33	122	126	201	203	434	428
Outflow Hydrograph (ac-ft)	0.33	0.33	156	158	562	570	3,858	3,884
Total Outflow and Floodplain Storage (ac-ft)	1,086	1,086	1,721	1,721	2,503	2,503	6,560	6,560

*Proposed Condition represents the full build out (including all areas to the north of the railroad and to the west of the main service complex. Partial build-out conditions results are not present here because they generally fall between the existing and proposed result, which are very similar.

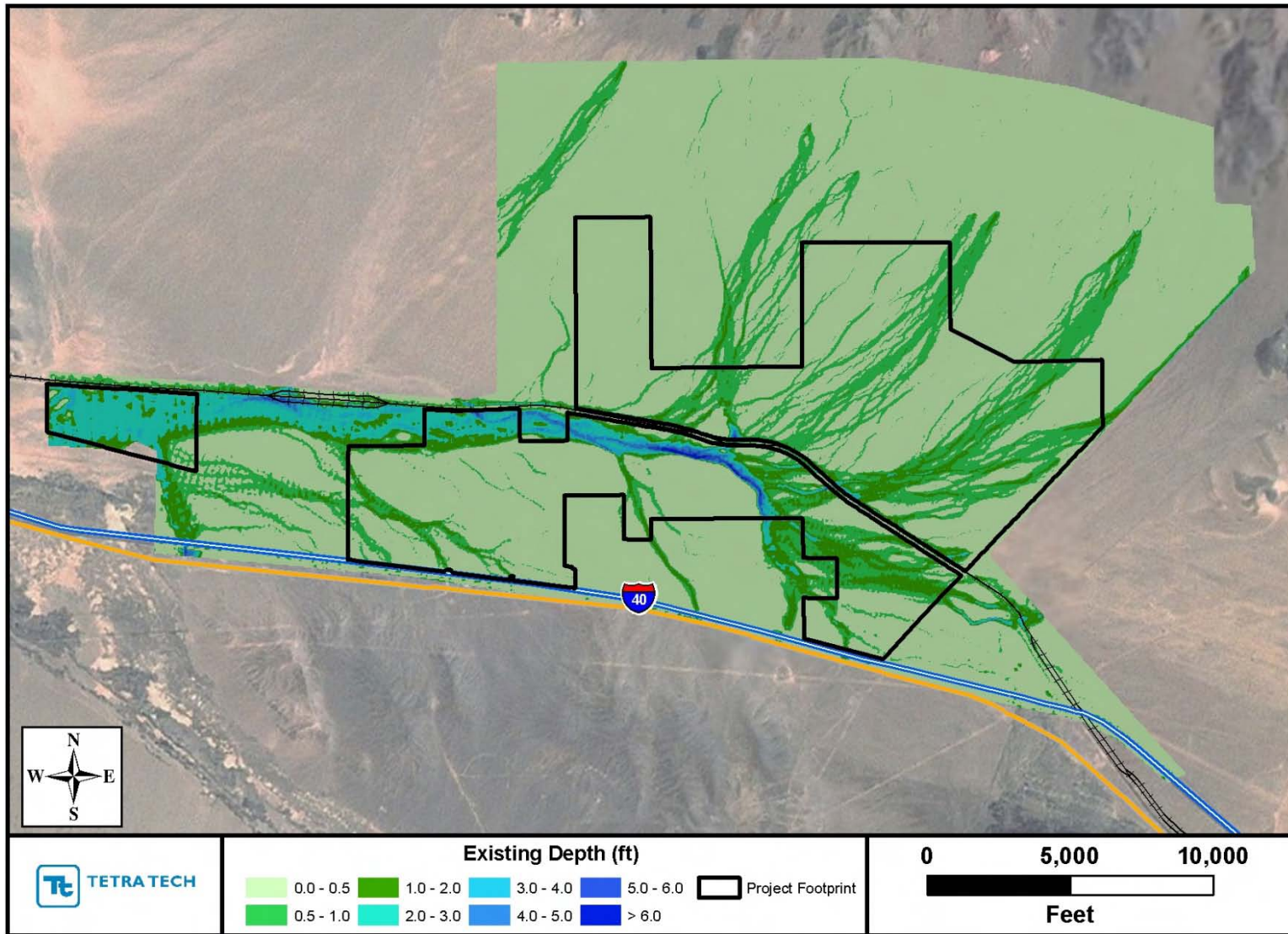


Figure 3.5a. Predicted maximum depth during 100-year, 24-hour storm under existing conditions.

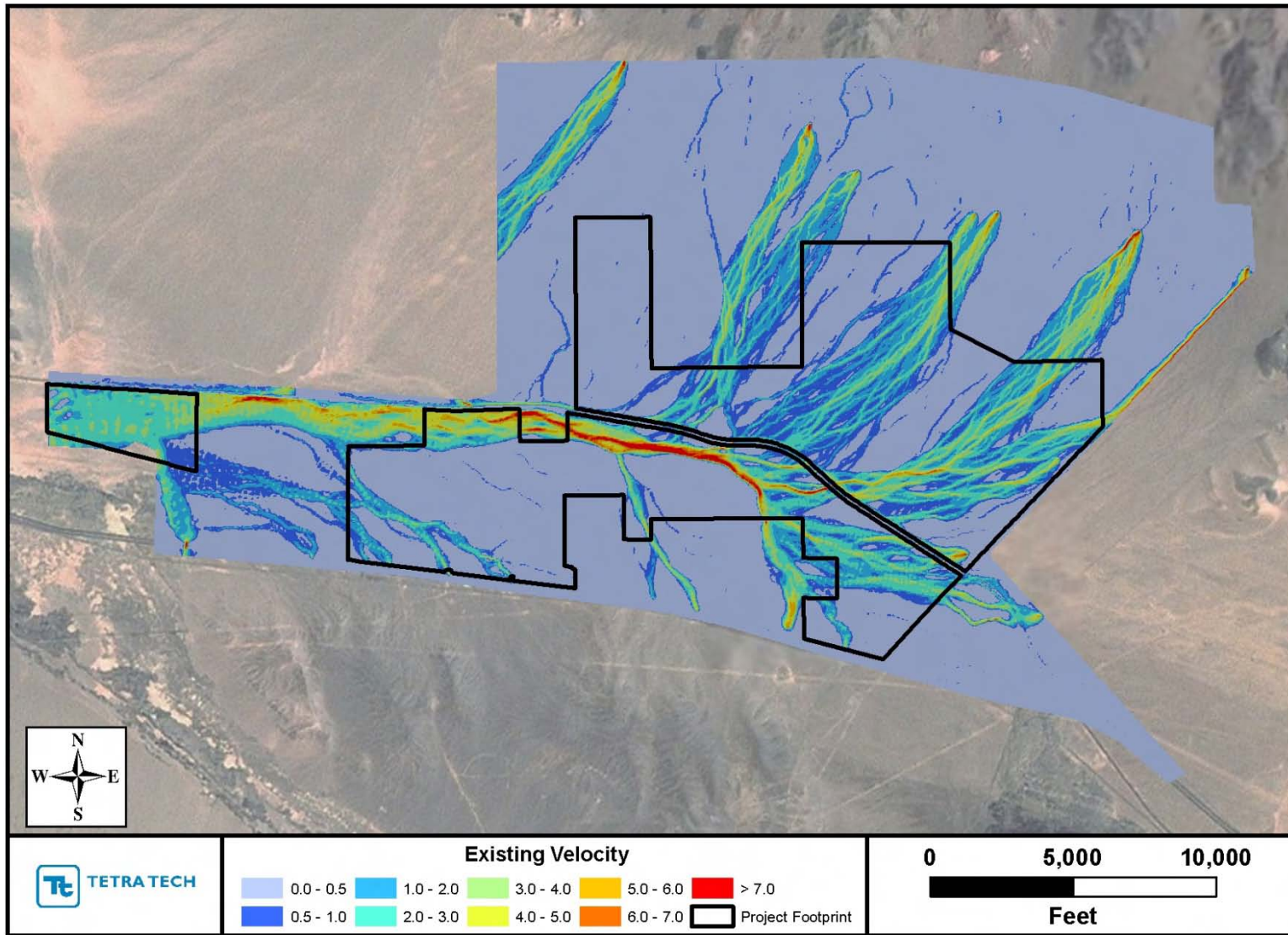


Figure 3.5b. Predicted maximum velocity during 100-year, 24-hour storm under existing conditions.

Table 3.6. Summary of predicted overtopping of the railroad line under existing conditions.				
Location	Recurrence Interval (years)	Depth (ft)	Duration (hrs)	Linear Extent (ft)
Near Trestle 5	100	0.6	6	810
Near Trestle 5	10	0.3	4	200
Near Trestle 6	100	0.5	6	240
Near At Grade Crossing	100	0.3	2	140
Near Trestle 9	100	0.5	30	270

interval and at only one location during the 10-year recurrence interval. More details about the extent and duration of overtopping are provided in the Infiltration Report (Tetra Tech, 2011).

3.3.2 Proposed Conditions

In general, the differences in overall model results for both partial and full build-out conditions from the existing conditions results for equivalent storms are insignificant (on the order of 1 percent or less for nearly all parameters), and well within the uncertainty of the analysis (Tables 3.3 and 3.4). For example, the overall time to peak discharge at all model grid cells averages 17.07 hours after the beginning of rainfall for the 100-year, 24-hour storm, and this decreases by only 0.03 hours (1.7 minutes) under proposed Project conditions. Similar, very small differences occur for the other modeled storms. Hydraulic conditions in specific areas of the site are, however, sufficiently different to warrant use of the Project conditions models for the site design. Minor differences also occur at some of the railroad drainage structures. Maximum depth and velocities throughout the site during the 100-year, 24-hour storm for full build-out conditions are shown in **Figures 3.6a and 3.6b**, and results for all modeled 24-hour storms are provided in **Appendix A**.

The small difference between existing and full build-out conditions at the railroad drainage structures is clearly illustrated by comparing the discharge and depth hydrographs at the Trestles 5 and 6 where some overtopping occurs during the 100-year, 24-hour storm, as discussed above (**Figures 3.7 and 3.8**). Although there are small variations in maximum flow depth on the upstream side of each of these drainage structures under Project conditions, the difference in overtopping discharge and water-surface elevations at the time of overtopping between existing and full build-out conditions is insignificant. The differences in predicted flows and overtopping conditions at the railroad drainage structures are described in more detail in the Infiltration Report (Tetra Tech, 2011).

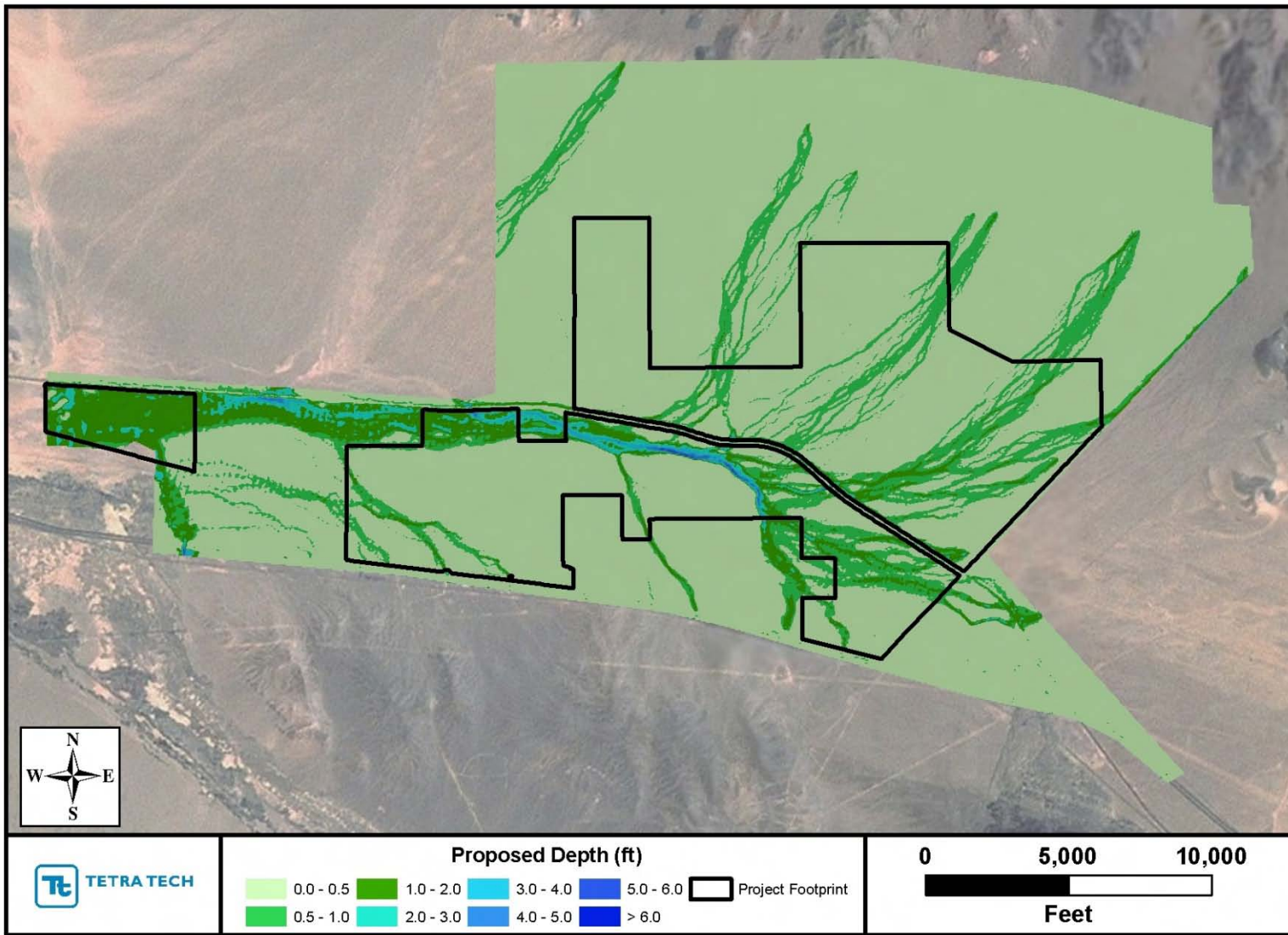


Figure 3.6a. Predicted maximum depth during 100-year, 24-hour storm under full build-out conditions.

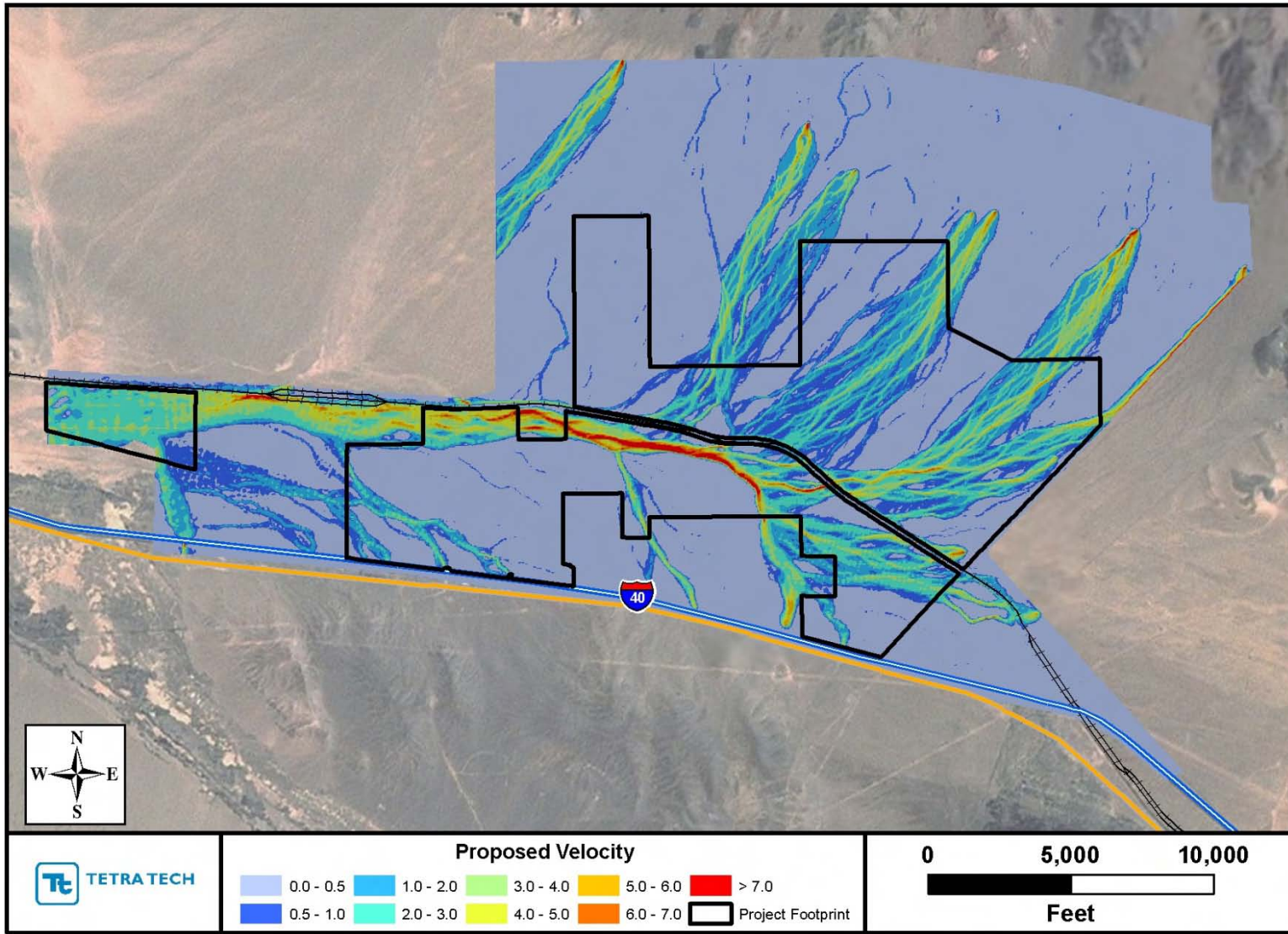


Figure 3.6b. Predicted maximum velocity during 100-year, 24-hour storm under full build-out conditions.

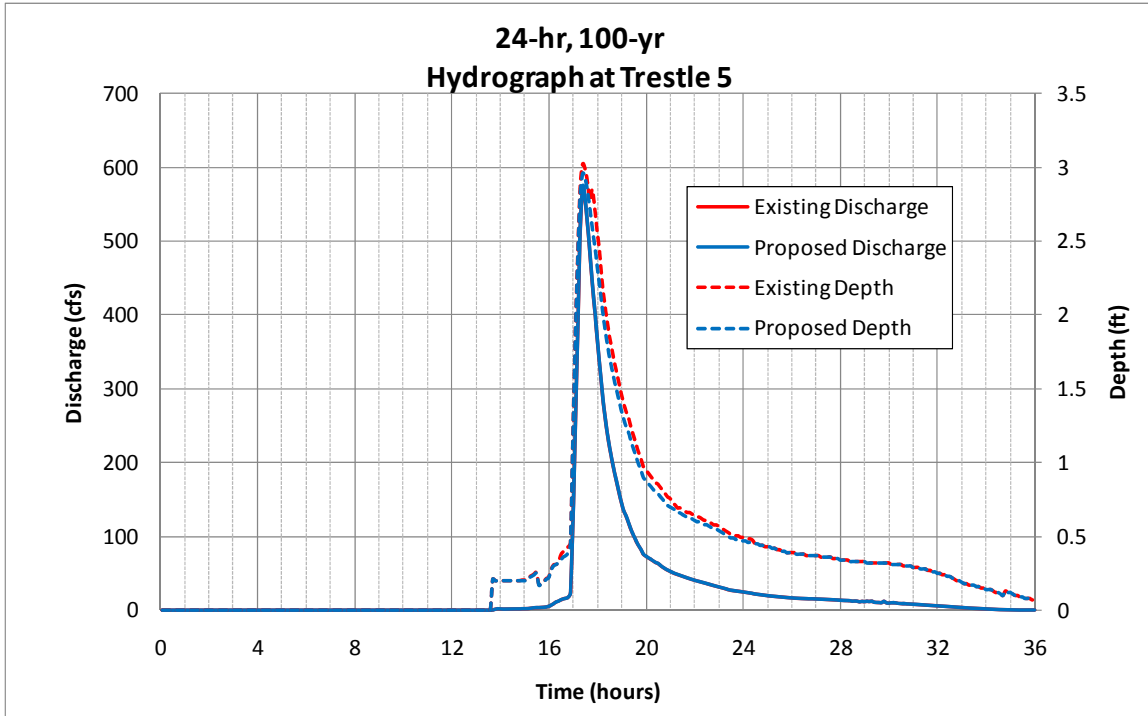


Figure 3.7. 100-year, 24-hour storm hydrographs at Trestle 5 under existing and full build-out conditions. NOTE: Existing and proposed discharges are nearly identical; thus, existing discharge line is covered by proposed discharge line.

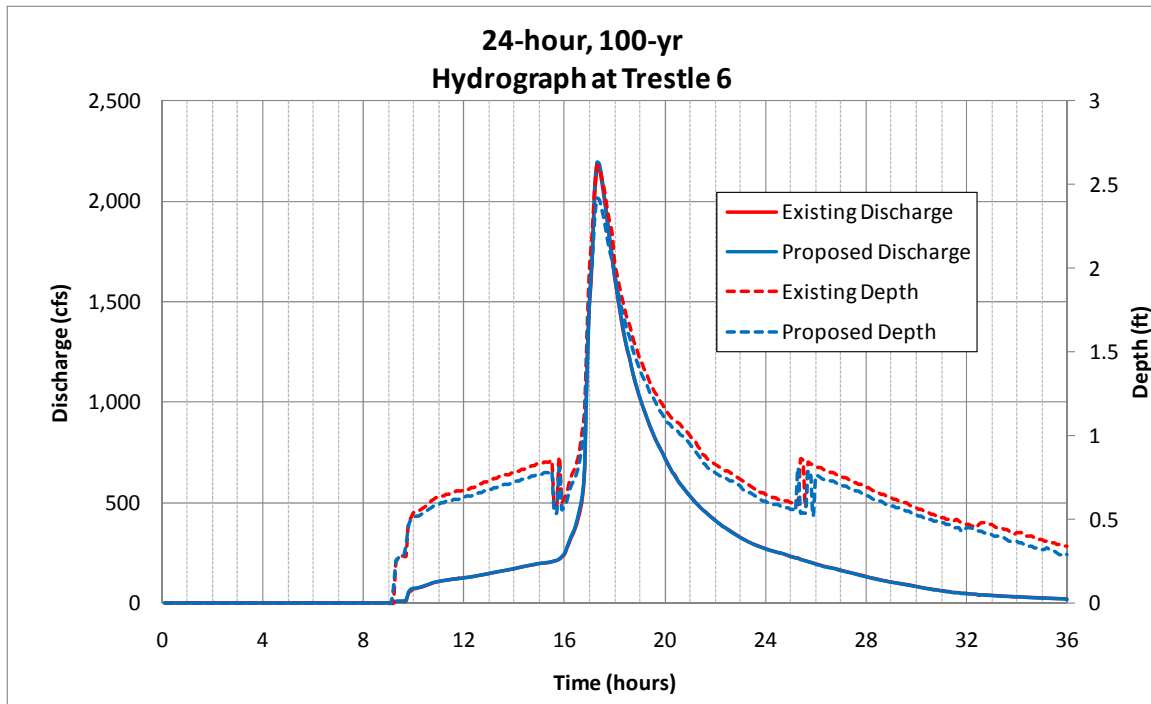


Figure 3.8. 100-year, 24-hour storm hydrographs at Trestle 6 under existing and full build-out conditions. NOTE: Existing and proposed discharges are nearly identical; thus, existing discharge line is covered by proposed discharge line.

4 SEDIMENT-TRANSPORT ANALYSIS TO ADDRESS GEOMORPHIC AND BIOLOGIC ISSUES

Hydraulic conditions from the FLO-2D model results were used to assess sediment transport rates at key locations throughout the site under existing and proposed (full build-out) conditions. As described in the previous section with respect to hydraulic conditions and below with respect to sediment transport conditions, the differences between existing and full build-out conditions are relatively small; thus, specific quantification of partial build-out conditions was not performed since the differences would be even smaller and would generally fall between the existing and full-build out results. The analysis was performed by extracting the hydraulic results for each of the modeled storms at key locations along the primary washes, estimating the bed material sediment transport capacities (i.e., sand and larger sediment) over the range of flows in each hydrograph, and assessing the differences in the transported sediment volumes for each storm between existing and full build-out conditions. Although a limited amount of fine sediment (i.e., silt and clay) would also be delivered from the upstream watershed and carried through the site, the quantities are relatively small due to the nature of the bedrock geology. This material (often referred to as *wash load*) is carried in suspension and does not interact in an important way with the bed of the washes; thus, it has little, if any, impact on the dynamics and stability of the washes throughout the majority of the site. For this reason, the fine sediment load was not considered in this analysis.

Bed-material transport capacities for each discharge at each of the identified locations were estimated using the Zeller-Fullerton (1983) equation, a power function relationship that was developed for channels with sand and gravel bed material that carry relatively low concentrations of wash load, and hydraulic conditions that are similar to those on the Project site. This equation is given by:

$$q_s = 0.0064 \frac{n^{1.77} V^{4.32} G^{0.45}}{Y^{0.30} D_{50}^{0.61}}$$

where q_s = unit width bed-material transport capacity (cfs/ft, unbulked),
 n = Manning roughness coefficient,
 V = velocity (fps),
 Y = flow depth (ft),
 D_{50} = median bed-material particle size (mm), and
 G = sediment gradation coefficient given by:

$$G = \left(\frac{D_{84}}{D_{50}} + \frac{D_{50}}{D_{16}} \right)$$

where D_{84} and D_{16} are the particle sizes for which 84 and 16 percent of the material is finer, respectively.

The total transport at any cross section (Q_s) is then given by $q_s * W$ where W is the width of flow at the location in question. A more detailed description of how this equation was developed and its range of applicability can be found in Mussetter Engineering, Inc. (2008), which can be accessed on-line at:

http://www.ssfac.com/development/documents/sediment_design_guide/Sediment%20Design%20Guide%2012-30-08.pdf.

The average gradation of the five samples that were collected along the upstream (north) boundary of the Project site was used for the transport capacity calculations at northerly analysis points, the average of Samples S5, S7 and S8 was used for the analysis locations in the vicinity of the railroad and in the main wash between the railroad and I-40, and a transitional gradation that was developed by averaging these two gradations was used for analysis points in the middle of the northern portion of the Project site (**Figure 4.1**). The particle size parameters and resulting coefficient of the Zeller-Fullerton equation are summarized in **Table 4.1**, and the locations of the analysis points and gradations applied to each are shown in **Figure 4.2**.

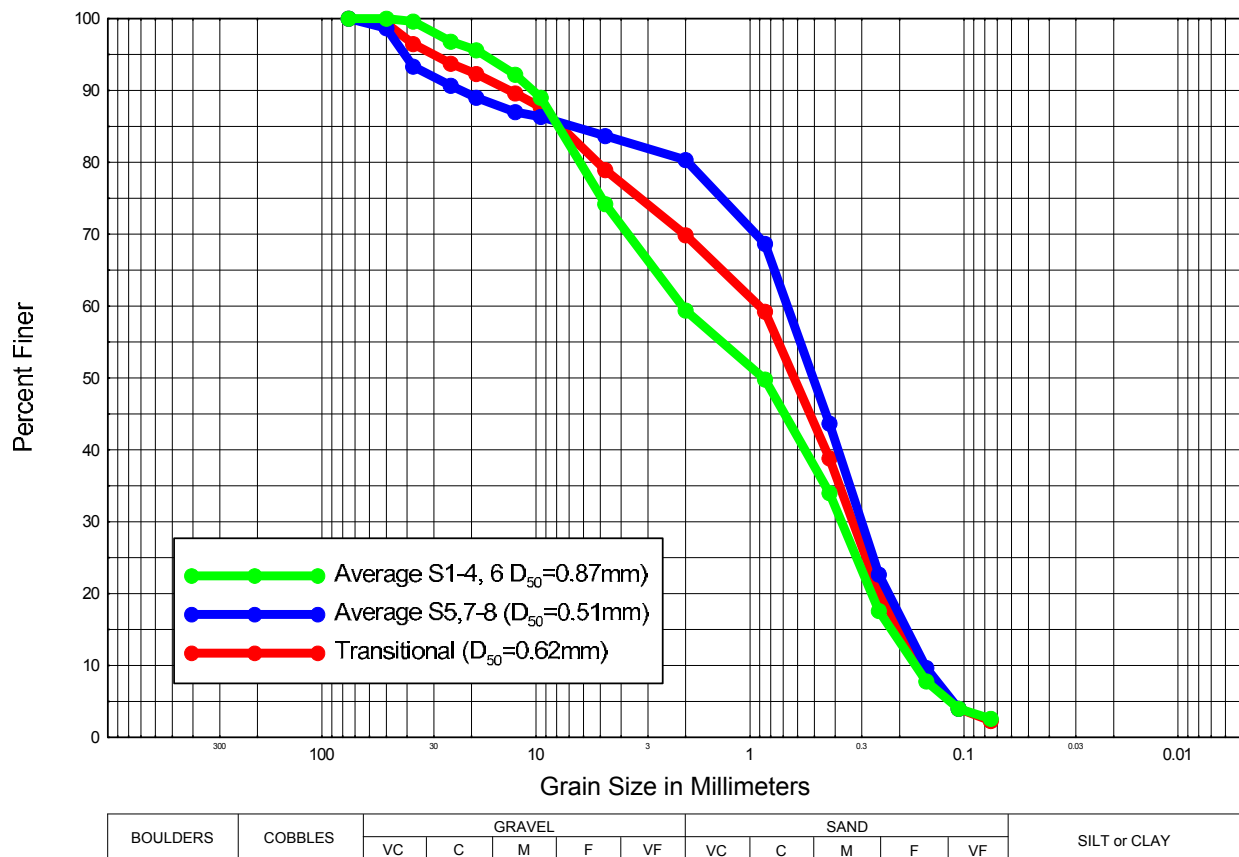


Figure 4.1. Bed-material sediment gradations used in the sediment-transport analysis.

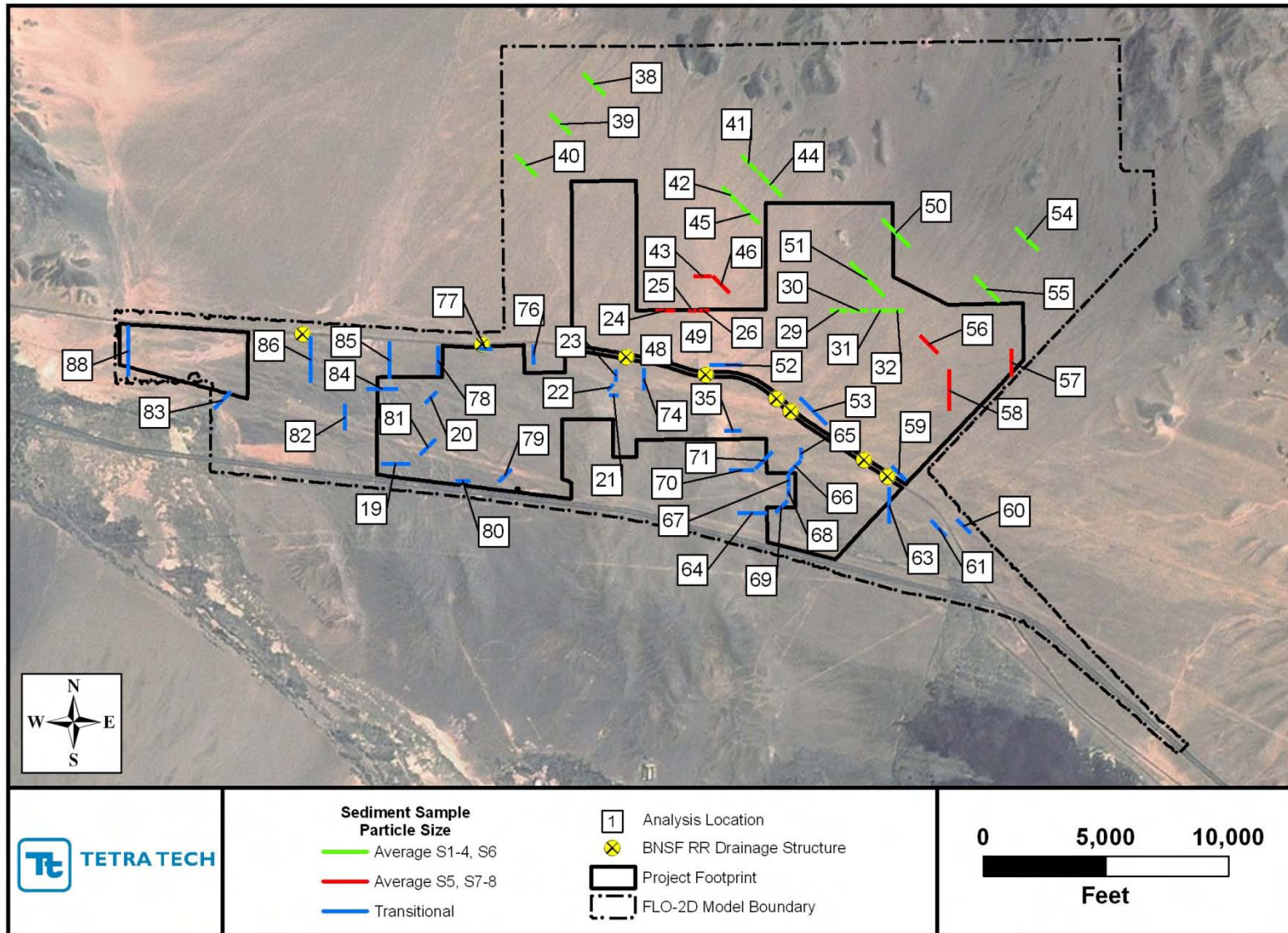


Figure 4.2. Location of sediment-transport analysis points and particle size gradation applied to each location.

The total quantity of bed material transported across the cross section lines at each of the analysis points in Figure 4.2 for each of the modeled storm was estimated by computing the transport capacity for each discharge in the hydrograph at that location and summing the individual transport capacities over the hydrograph. For purposes of validating the results, total quantity of sediment entering the Project site from the north was estimated by adding the results for Analysis Points (AP) 24, 25, 26, 50, 55 and 57 for each of the modeled storms. The average annual sediment load to these points was then computed by integrating the individual storm totals over the flood frequency curve using the following equation (Mussetter Engineering, Inc., 2008):

$$Y_s \text{ (average annual)} = 0.015Y_{s100} + 0.015Y_{s50} + 0.04Y_{s25} + 0.08Y_{s10} + 0.2Y_{s5} + 0.4Y_{s2}$$

where Y_{si} is the sediment yield for each individual storm event. The resulting average annual yield was compared with average sediment yields reported by Griffiths et al. (2006) (**Figure 4.3**). The watersheds considered by Griffiths et al. (2006) ranged from about 0.015 km² to about 0.15 km², and the average annual sediment yield varied from about 35 metric tons/km² to 19 metric tons/km², with the typical trend of decreasing sediment yield with increasing drainage area. The cumulative drainage area contributing to the above six analysis points is approximately 28 km², and the estimated average annual sediment yield from the sediment transport calculations is about 13 metric tons/km². This value is very consistent with and fits the trend of the data from Griffiths et al. (2006).

The differences in sediment loads to the railroad drainage structures between existing and proposed conditions were assessed by computing the transport quantities for the individual storms using the above procedures for AP 77, AP 48, AP 52, AP 53, AP 59 and AP 60 (**Figure 4.4**). As shown in Figure 4.4, the differences are relatively insignificant. With the exception of AP 77, the model results indicate that the average annual sediment load actually decreases under project conditions at all locations except AP 77 (Drainage Structure 2) by a few percent. Considering the overall uncertainty in sediment transport calculations, in general, this difference is more likely the result of variability in the results due to the numerical tolerances in the model than an indication of a real change. The estimated sediment loads to AP 77 are about 15 percent higher under proposed conditions than under existing conditions, however, detailed evaluation of the computations indicates that a single discharge in the output file at the beginning of surface runoff at this location is anomalously high, and this discharge is the cause of essentially all of the difference in transport rates. The majority of the data points that fall above the line of equal agreement in Figure 4.6 are associated with this analysis point; thus, this relatively small difference is not believed to represent a real increase in sediment loads at this point.

A similar comparison was performed for the other analysis points shown in Figure 4.2 (**Figure 4.5**). These results indicate that the sediment loads in other areas of the site are also very similar between existing and proposed conditions, with nearly an equal number of locations experiencing a decrease in load as experience an increase. Most of the differences seen in Figure 4.5 are related to anomalous discharges in the model output that tend to skew the results, as discussed above. At the downstream model boundary, predicted sediment loads actually decrease by about 20 percent due to a slight decrease in the discharge.

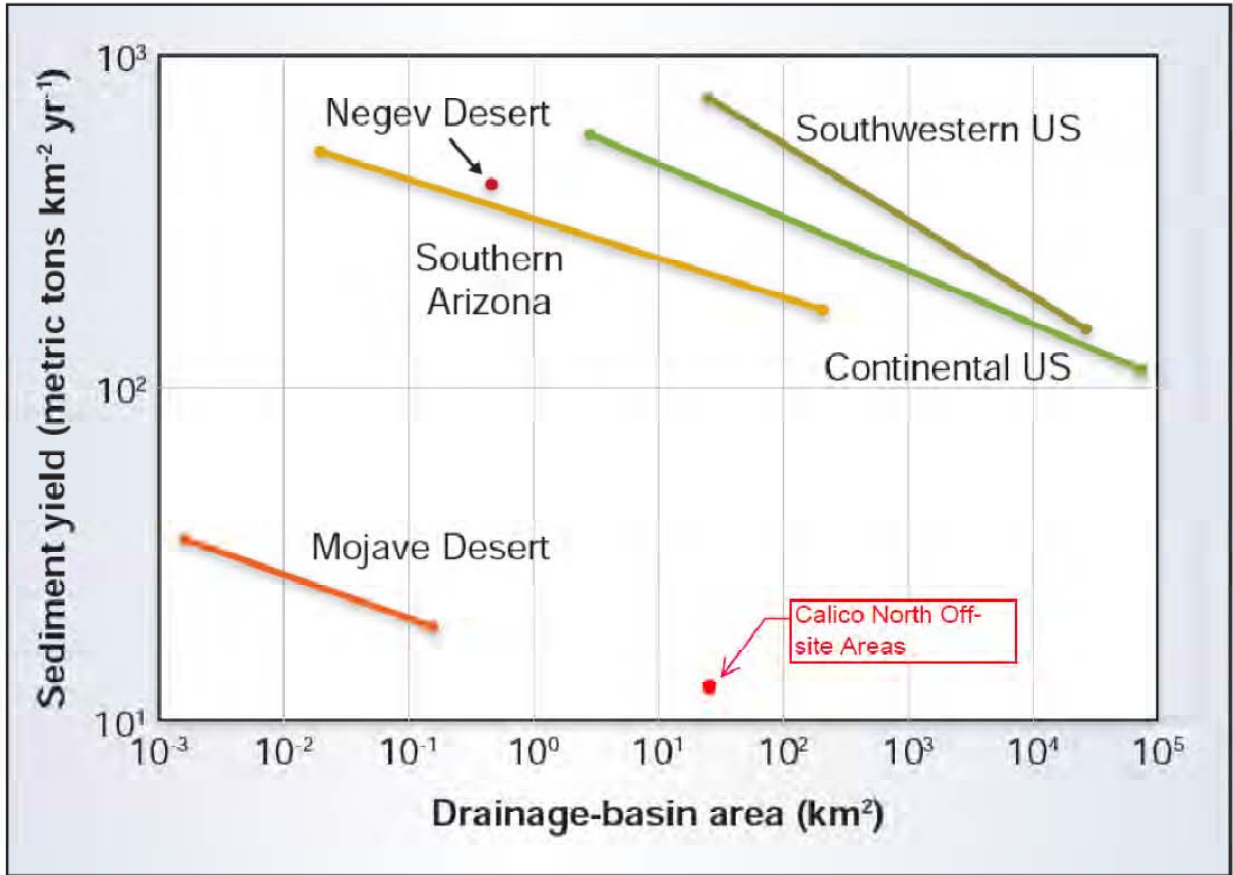


Figure 4.3. Graph showing the relation between sediment yield and drainage area for drainage basins in five different locations. Note that the Mojave Desert drainage basins generate an order of magnitude less sediment per unit area than basins elsewhere (modified from Griffiths et al., 2006).

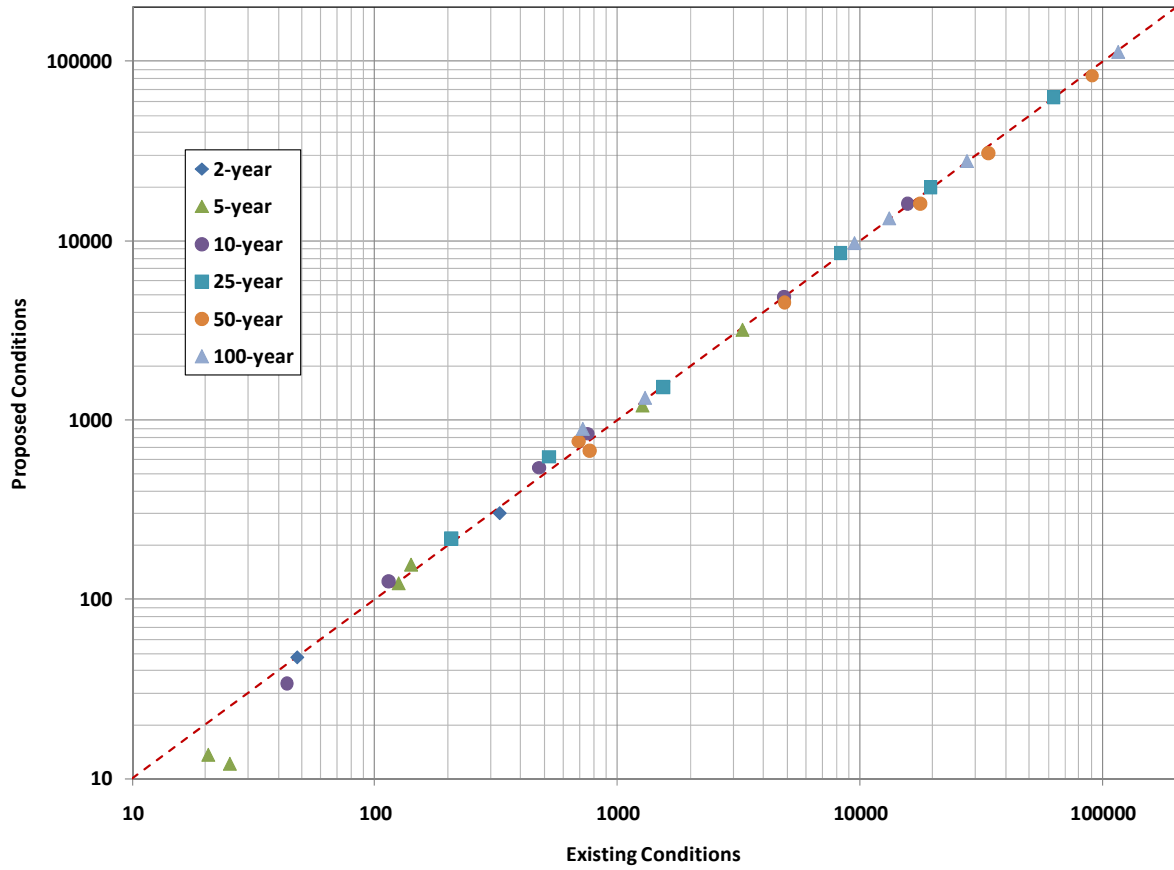


Figure 4.4. Comparison of total bed-material sediment loads for the 2- through 100-year storm hydrographs in the washes just upstream from the BNSF Railroad line (AP 77, AP 48, AP 52, AP 53, AP 59 and AP 60). Points falling below the red line indicate a decrease in sediment load under proposed conditions; points above the line indicate an increase in sediment load.

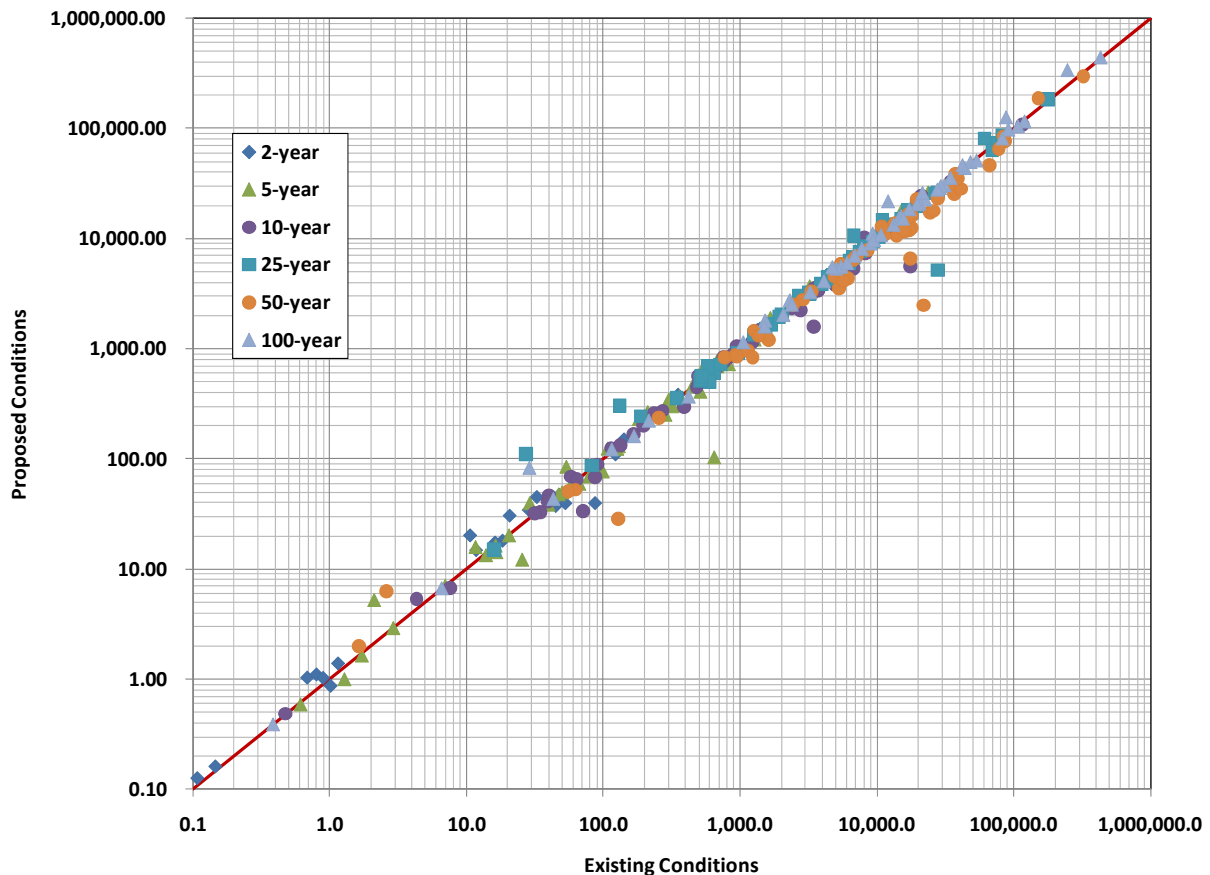


Figure 4.5. Comparison of total bed-material sediment loads for the 2- through 100-year storm hydrographs in the washes at the analysis points shown in Figure 4.2 (except those shown in Figure 4.4). Points falling below the red line indicate a decrease in sediment load under proposed conditions; points above the line indicate an increase in sediment load.

In general, these results indicate that the proposed project will have an insignificant effect on the movement of sediment through the site, both in terms of the complete gradation of bed material that is important to channel stability and the finer size-fractions that are the source of material for the sensitive MFTL dune habitat. The results presented indicate that the proposed project will not have a measurable effect on the overall sediment balance on and downstream from the project site. This is true regardless of whether a particular year is an El Niño or La Niña year. The processes of greater precipitation and more intense monsoonal storms associated with El Niño conditions and less precipitation and generally less intense monsoonal storms during La Niña conditions, and their attendant effects on the availability of fine sand to maintain Aeolian dunes will also continue to operate as they have historically.

Although the overall sediment balance will not be affected, some local scour could be induced by the abrupt transition between compacted and uncompacted areas, such as the secondary access roads and the drainage structures through the main access road. These local instabilities are not expected to cause systematic instability of the existing washes nor will they change the overall sediment balance within the site unless they are allowed to develop over multiple storms. This can be prevented by systematic inspection of the project area after runoff producing events in the course of other maintenance activities, and any local instabilities corrected in a timely manner by installing local protection measures.

5 SUMMARY AND CONCLUSIONS

An analysis was conducted to assess the potential effect of the proposed Project on the transport of bed material-sized (sand and coarser) sediment onto and through the Project site. The analysis met two specific objectives:

1. An assessment of the potential for the project to change the overall sediment balance within the site that could affect the stability of the existing washes and drainage pathways in a manner that could negatively impact the safety of infrastructure on and near from the Project site, including the BNSF Railroad line and associated drainage structures, and
2. An assessment of the potential for the project to affect the quantity of fine sand that is available for Aeolian transport from the washes to maintain existing sensitive dune habitat for the Mojave Fringe-toed Lizard (MFTL).

The analysis was conducted by estimating the bed material transport capacity at a range of locations on the site using hydraulic information from the FLO-2D model described in detail in (Tetra Tech, 2011) with a bed material transport capacity equation applicable to conditions at the site. The Zeller-Fullerton (1983) equation was chosen for the analysis from the numerous equations that are available in the literature because it was developed for conditions similar to those at the Project site, it has been successfully applied to similar analyses on many previous projects, and the resulting average annual sediment yields are consistent with measured sediment yields in the Mojave Desert. The bed material particle size gradations used in the analysis were derived from samples collected by Tetra Tech in 2011. These gradations indicate that the alluvium on the fan/bajada surface in the upstream portion of the site north of the BNSF Railroad consists of about 60-percent sand, 40-percent gravel and a small amount (generally less than 2 to 3 percent) silt and clay, and the material fines in the downstream direction to about 70-percent sand, 20-percent gravel and a small amount of silt and clay near the railroad and along the valley floor between the railroad and I-40. Aeolian sand that is important to the MFTL habitat is typically in the range of 0.4 mm, and this size-range comprises about 34 percent of the material in the upstream (north) part of the site, increasing to about 40 percent in the vicinity of the railroad and between the railroad and I-40.

The project design is specifically intended to minimize effects on the existing washes and drainageways by constructing the secondary access roads at grade, providing appropriately-sized drainage structures through the main access road, and supporting the PV arrays and SunCatchers™ on posts that have as small a footprint as possible. The effects of the features on hydraulic conditions during the 2- through 100-year storms was evaluated by incorporating information into the model input files to represent the effect of these features on infiltration rates, hydraulic roughness and decreased flow area due to the presence of the support posts and other project features. As described in detail in the Infiltration Report (Tetra Tech, 2011), the effect of the project features on hydraulic conditions on the site over the range of modeled flows is relatively insignificant. As a result, the sediment-transport analysis also indicates that the project will have a relatively insignificant effect on the movement of sediment across the site, although differences in excess of 20 percent occur at specific locations. Results for analysis points immediately upstream from the BNSF Railroad indicate that the amount of sediment delivered to the railroad drainage structures under proposed conditions is nearly identical to existing conditions, and the overall sediment balance within the site is also nearly identical.

In assessing these results, it is important to understand that the relationship between sediment transport capacity and the local hydraulic conditions for the physical setting at the project site is highly non-linear [e.g., the sediment transport capacity is typically proportional to the velocity raised to the 3 to 5 power, and specifically, the 4.3 power in the Zeller-Fullerton (1983) equation]. As a result, minor changes in the hydraulic conditions are magnified in the sediment transport capacity estimates. Under field conditions, a significant amount of the variability in transport capacity from one location to the next (and also resulting from minor changes in the hydraulic conditions among alternatives) would be dampened by local sorting of the bed material; thus, the variability in transport rates indicated by the numerical calculations would not actually occur under field conditions. In addition, although some of the differences that are seen at the analysis points result from minor changes in the hydraulic conditions associated with project features, many appear to be related to variability in the model output for nearly identical conditions that result from tolerances in the numerical solution methods employed in the model, and these differences are not a real indication of project effects.

As noted above, local instabilities could occur at the abrupt transition between compacted and uncompacted areas, such as the secondary access roads and the drainage structures through the main access road. These areas are not expected to cause systematic instability of the existing washes nor will they change the overall sediment balance within the site unless they are allowed to develop over several storm events. It is recommended that the site be inspected after runoff-producing events, and any localized instabilities corrected by installing local protection measures prior to the next storm.

6 REFERENCES

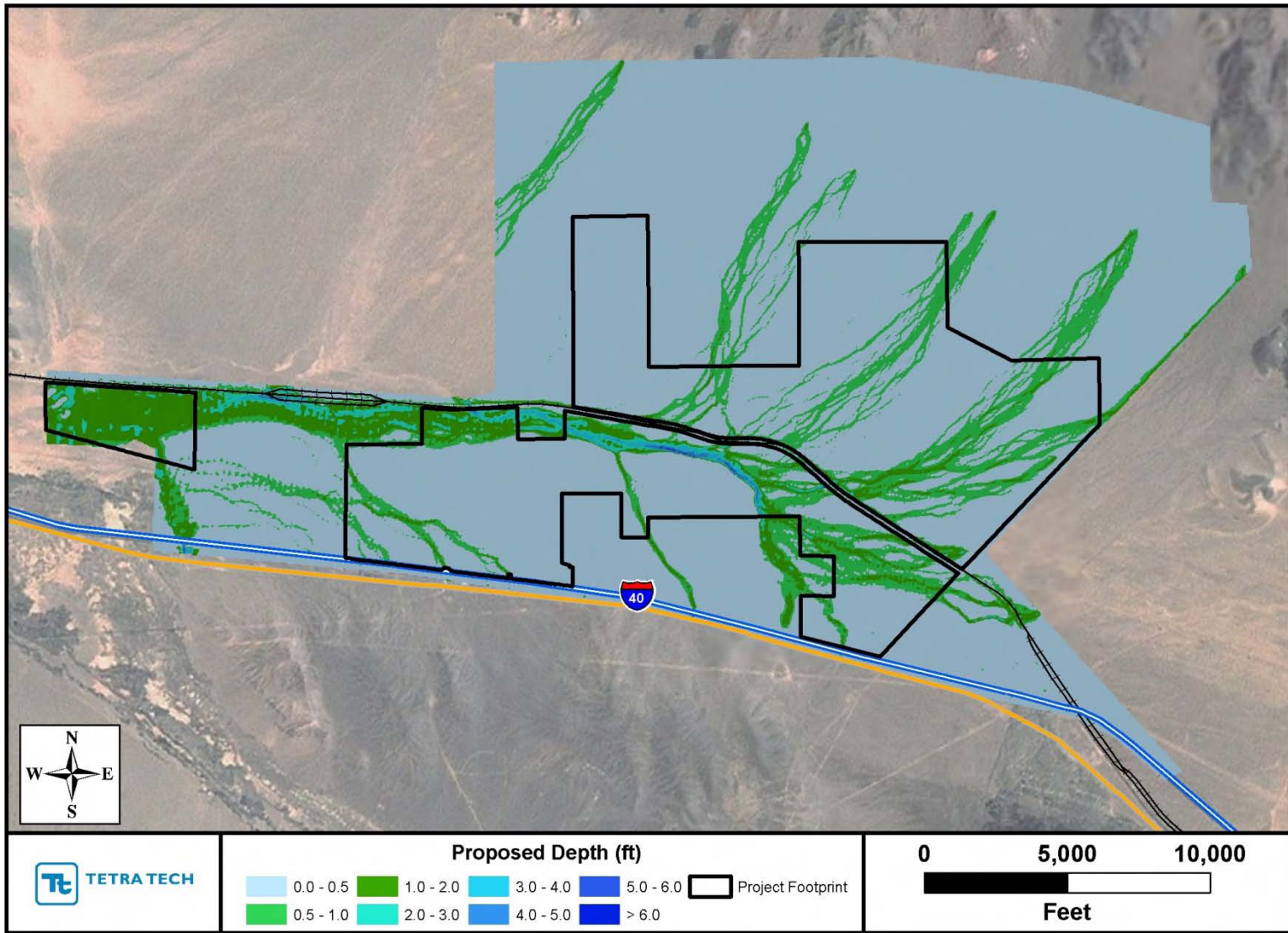
- Blakemore, E.T., Hjalmarson, H.W., and Waltemeyer, S.D., 1997. Methods for Estimating Magnitude and Frequency of Floods in the Southwestern United States. U.S. Geological Survey Water-supply Paper 2433, 206 p.
- Bureau of Land Management, 2010. Final Environmental Impact Statement and Proposed Amendment to the California Desert Conservation Area Plan for the Calico Solar (formerly SES Solar One) Project, San Bernardino County, California, August, 787 p.
- Cayan, D.R., Redmond, K.T., and Riddle, L.G., 1999. ENSO and hydrologic extremes in the western United States. *Journal of Climate*, v. 12, pp. 2881-2893.
- Dillon Consulting Limited, 2011. 2176047 Solar Energy Project Stormwater Management Report. Prepared for UC Solar Ltd. And Canadian Solar Solutions, May 18, 17 p.
- FLO-2D Software, Inc., 2009. FLO-2D model. Documentation and software available online at: www.flo-2d.com.
- Griffiths, P.G., Hereford, R., and Webb, R.H., 2006. Sediment yield and runoff frequency of small drainage basins in the Mojave Desert, California and Nevada. U.S. Geological Survey Fact Sheet 2006-3007, 4 p.
- Hereford, R, Webb, R.H., and Longpre, C.I., 2004. Precipitation History of the Mojave Desert Region, 1893-2001. U.S. Geological Survey Fact Sheet 117-03, 4 p.
- Holland, R.F. 1986. Preliminary Description of the Terrestrial Natural Communities of California. CDFG.
- Huitt-Zollars, 2009. Existing conditions hydrologic and hydraulic study for Solar One (Phase 1 and 2) Project Site, Binder Two. Prepared for Stirling Energy Systems, Inc., pp. 98-143.
- Mantua, N.J. and Hare, S.R., 2002. The Pacific decadal oscillation. *Journal of Oceanography*, v. 58, pp. 35-42.
- Mussetter Engineering, Inc., 2008. Sediment Design Guide. Prepared for the Southern Sandoval County Arroyo Flood Control Authority, Rio Rancho, New Mexico, November, 246 p.
- Natural Resources Conservation Service (NRCS), 1986. Urban Hydrology for Small Watersheds. Technical Release 55, June, 164 p.
- NOAA Climate Prediction Center, 2011. Cold and warm episodes by season: Changes to the Oceanic Niño Index (ONI), 1950-2011.
- Philip Williams & Associates, Ltd., 2010. Geomorphic Assessment of Calico Solar Project Site: Appendix A (Biology Report). Prepared for the California Energy Commission, July 9, 30 p.
- Pima County Department of Transportation and Flood Control District (PCDOT&FCD), 1979. Hydrology Manual for Engineering Design and Flood Plain Management Within Pima County Arizona. Written by Zeller, M.E., Tucson, Arizona, September.
- San Bernardino County, 1986. Hydrology Manual. Prepared by Williamson and Schmid, Civil Engineers, Irvine, California, August, 207 p.
- San Bernardino County, 2010. Hydrology Manual Addendum for Arid Regions, April, 6 p.

- SES. 2009. URS/C. Lytle (tn 54619). Biological (Bio) Resources Technical (Tech) Report (Rpt), Noxious Weed Management (Mgmt) Plan, Biological (Bio) Resources Baseline Survey. Submitted to CEC/Docket Unit on December 23.
- Soil Survey Staff, Natural Resources Conservation Service, U.S. Department of Agriculture. U.S. General Soil Map (STATSGO2). Available online at <http://soildatamart.nrcs.usda.gov>, accessed August 2011.
- Steinberger, D.P., 2010 Solar Panels Not Impervious Cover in New Jersey. Environmental & Energy Law Monitor, May 3, 1 p.
- Tetra Tech, 2011. Calico Solar Project Infiltration Report. Submitted to K Road Calico Solar LLC, Berkeley, California, September 6, 200 p.
- Thomas, B.E., Hjalmarson, H.W., and Waltemeyer, S.D., 1997. Methods for Estimating Magnitude and Frequency of Floods in the Southwestern United States. U.S. Geological Survey Water-Supply Paper 2433, 205 p.
- URS, 2009. Sediment Transport Analysis Sampling, Solar One Project. URS Project Number 27658105.05000, memorandum prepared for Tessera Solar/SES, March 23.
- Woodward, D.E., 1973. Runoff curve numbers for semiarid range and forest conditions. Presentation to 1973 Annual Meeting of the American Society of Agricultural Engineers, Lexington KY, June 17-20, 14 p.
- WRCC (Western Regional Climate Center). 2010. Western U.S. Climate Historical Summaries. Report for Daggett FAA Airport, California (042257). <http://www.wrcc.dri.edu/cgi-bin/cliMAIN.pl?ca2257> (accessed June 15, 2011).
- Zeller, M.E., 1993. Curve Number Equations for 24-hour Storms. Prepared for Pima County Flood Control District, May, 2 p.

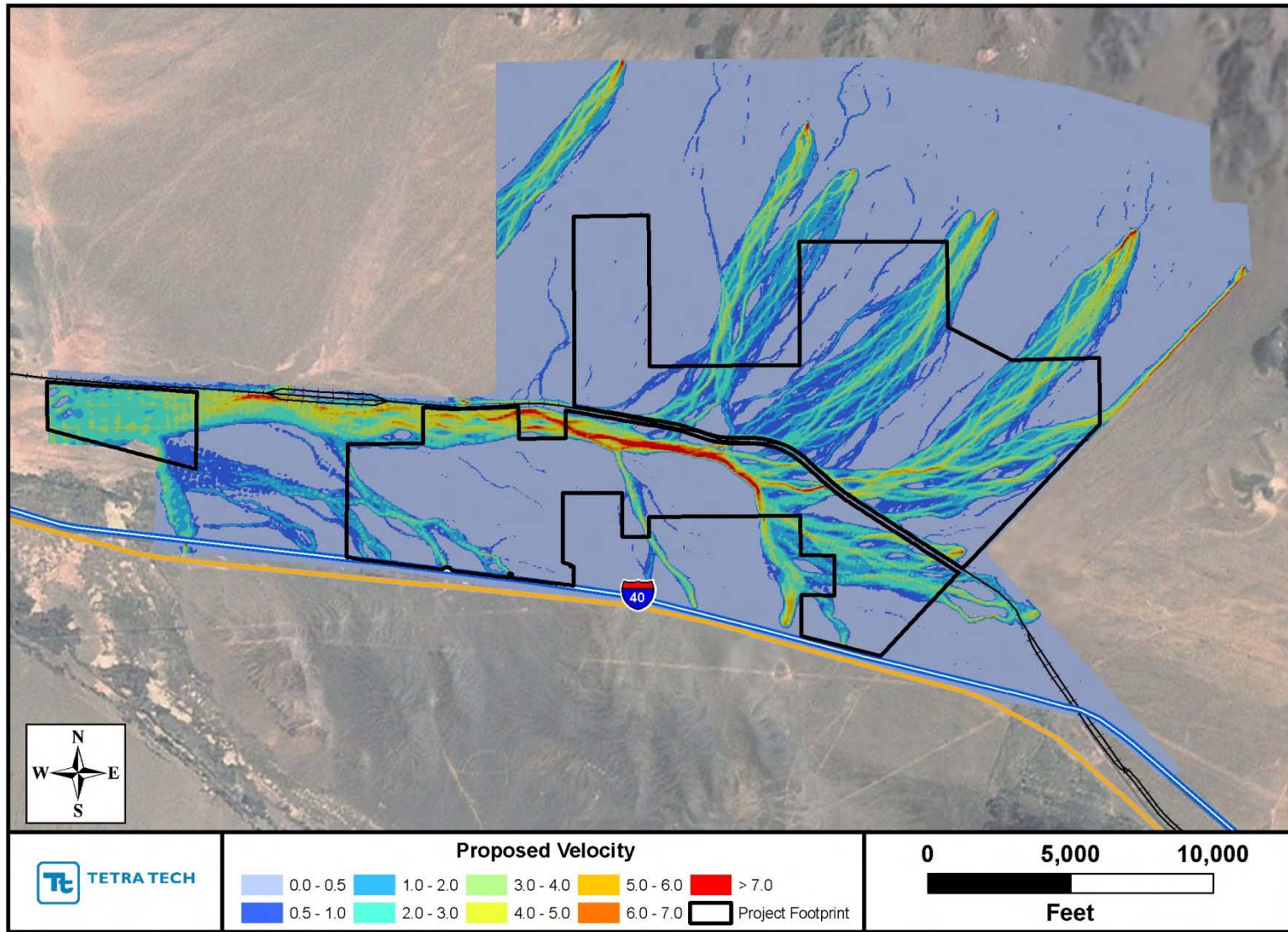
APPENDIX A

Depth and Velocity Distribution Maps for Full Build-out Conditions for the 100-, 50-, 25-, 10-, 5- and 2-year Storms

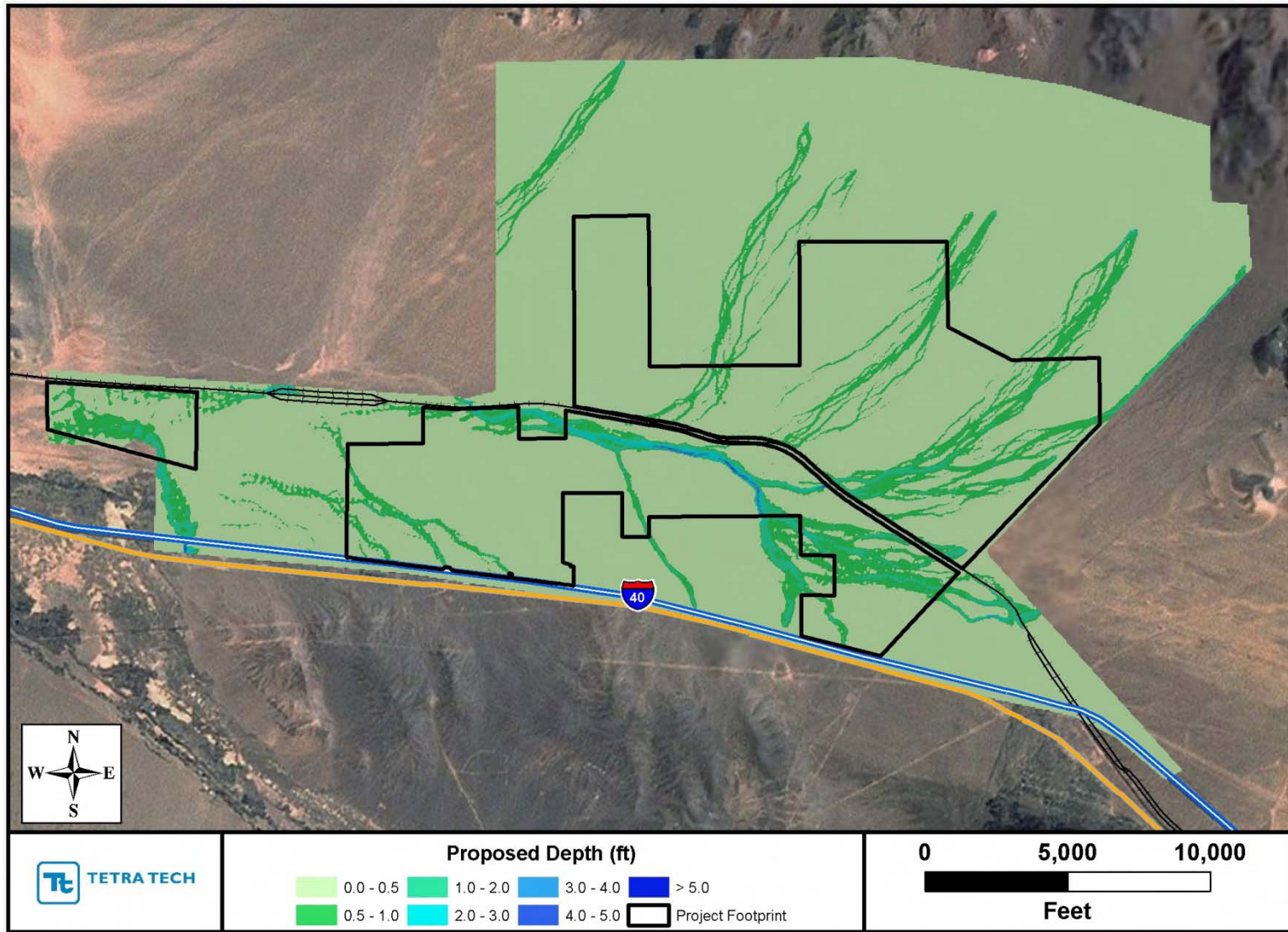
**(Note: The color gradient scale on the 2- through 25-
year are different from the 50- and 100-year)**



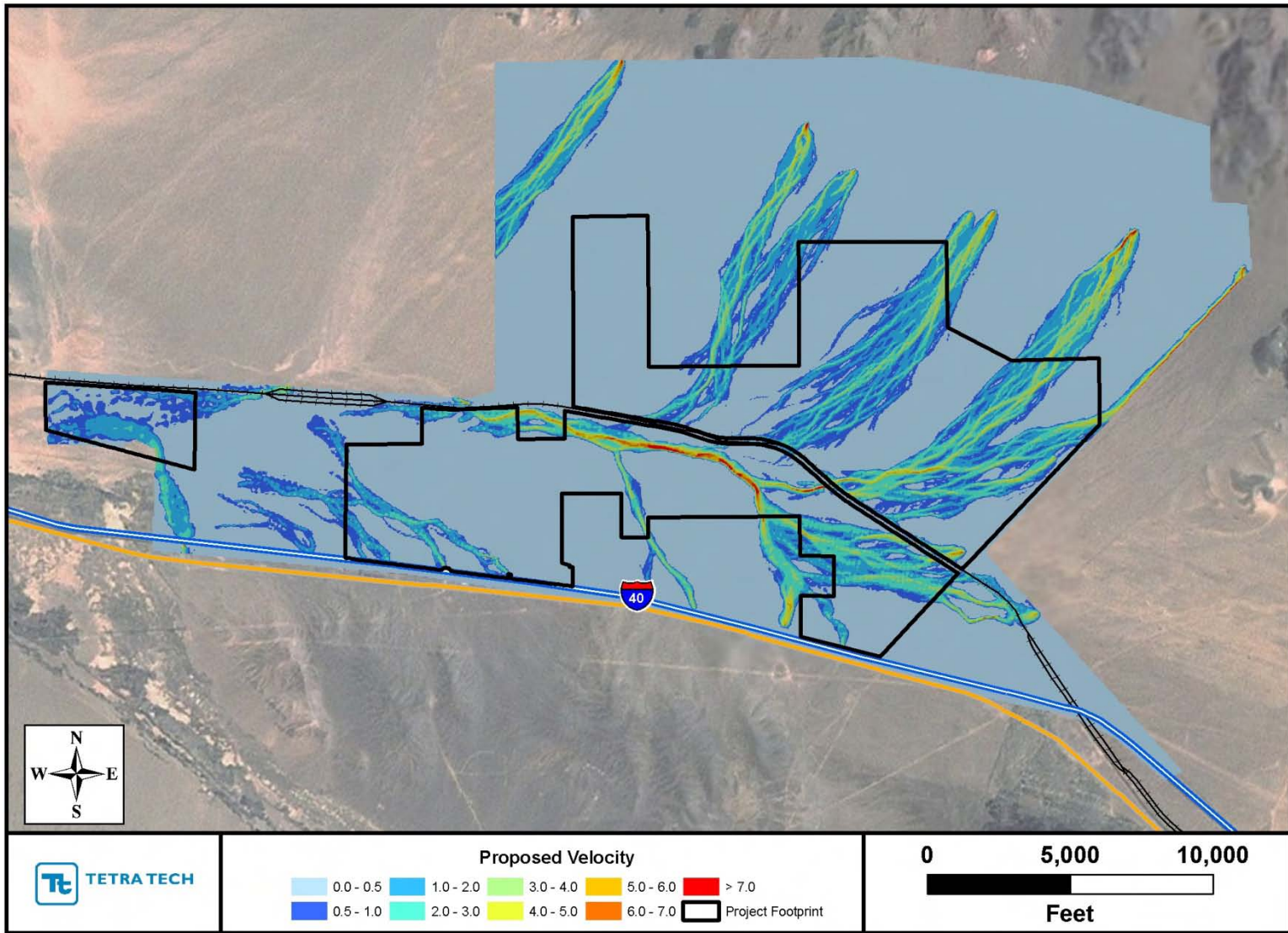
Maximum depths during the 100-year, 24-hour storm.



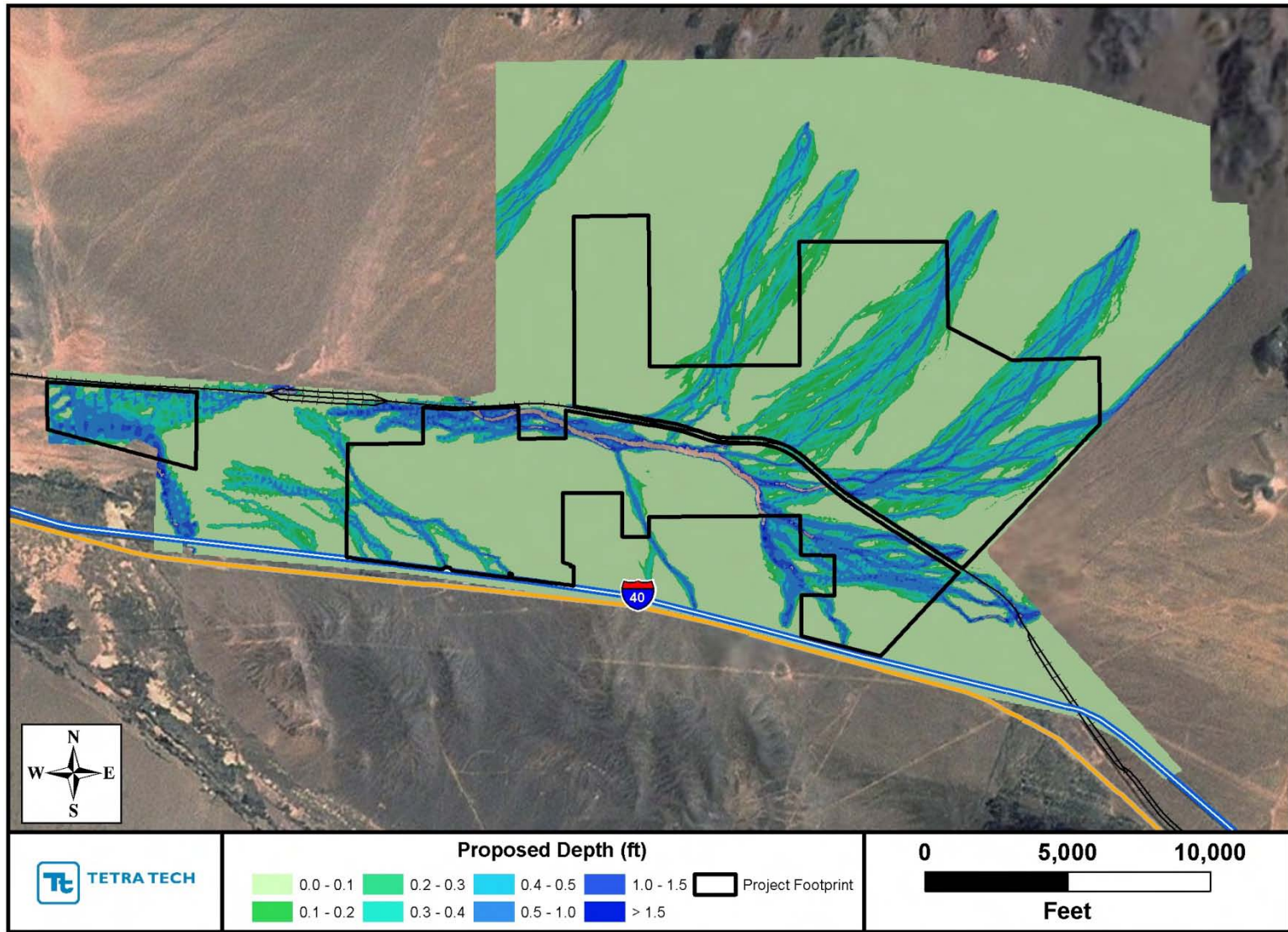
Maximum velocity during the 100-year, 24-hour storm.



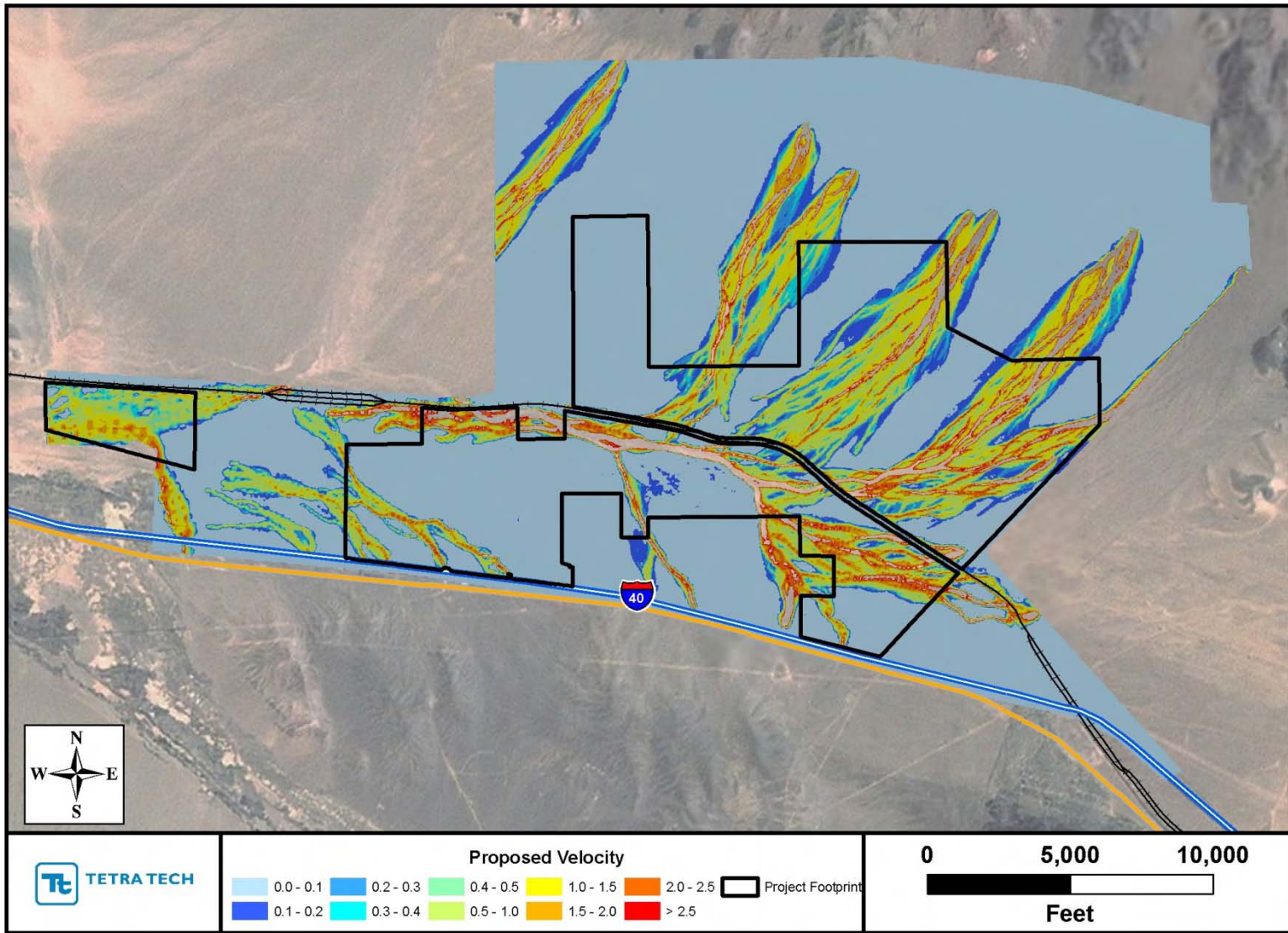
Maximum depths during the 50-year, 24-hour storm.



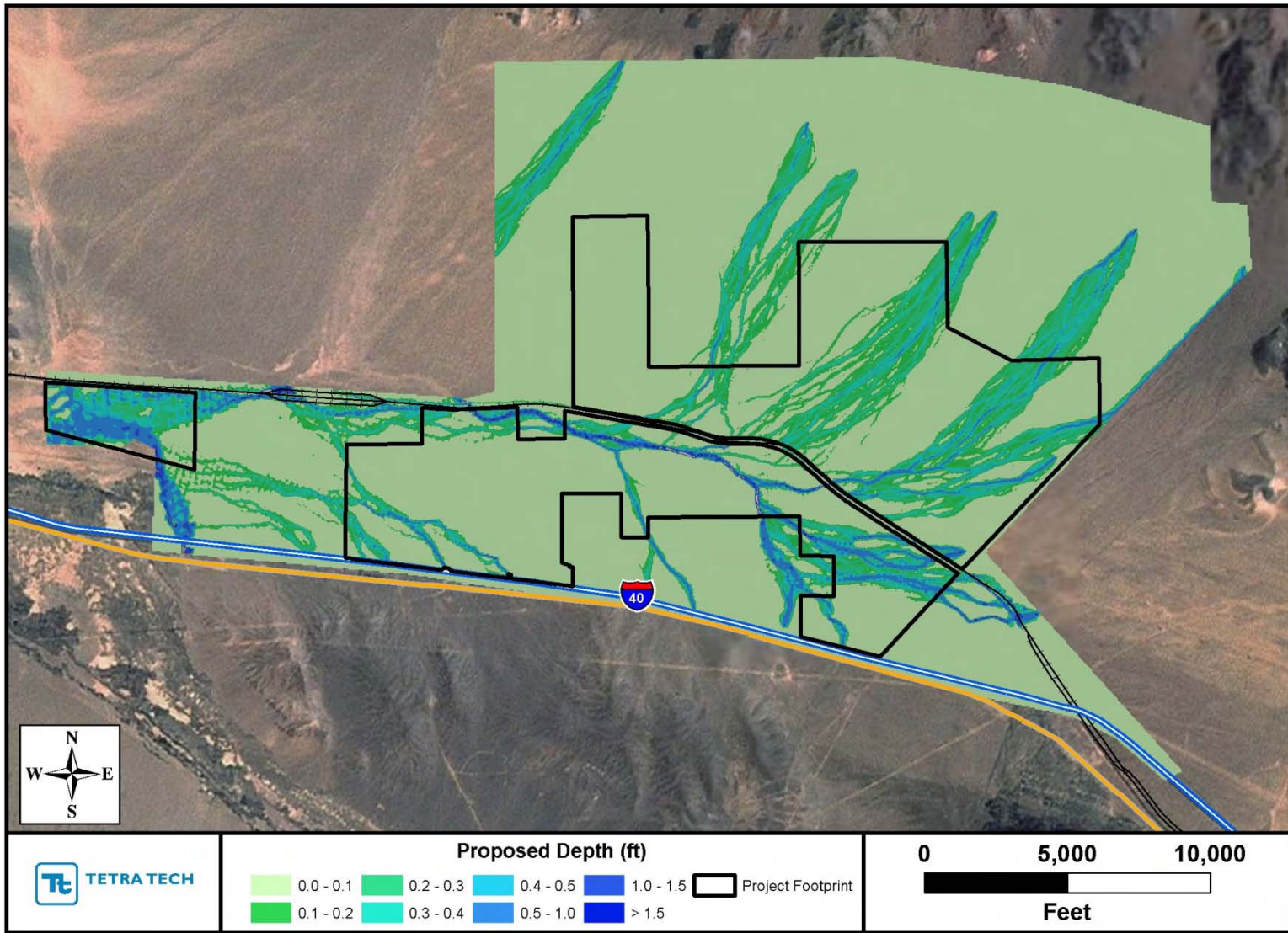
Maximum velocity during the 50-year, 24-hour storm.



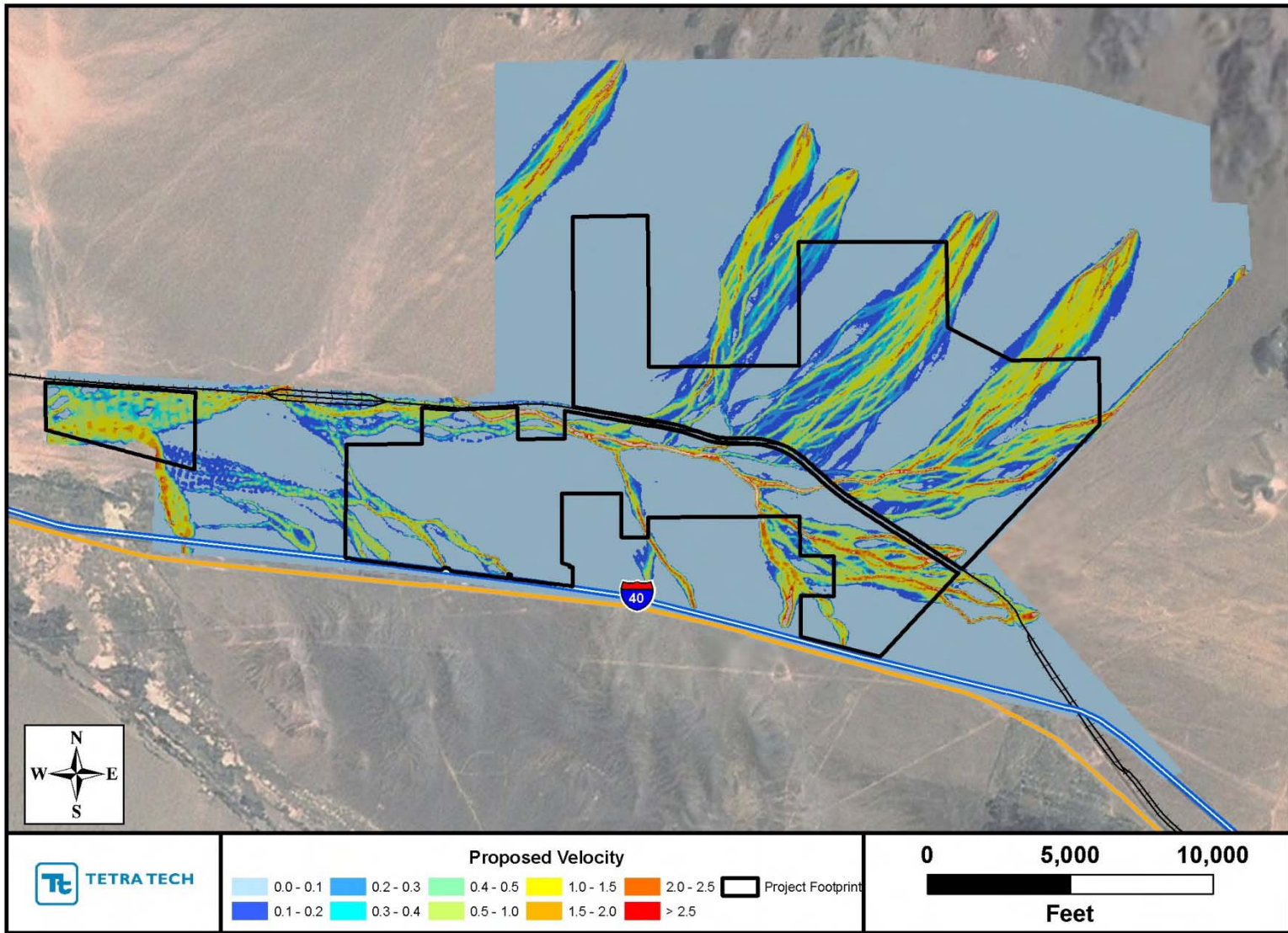
Maximum depths during the 25-year, 24-hour storm.



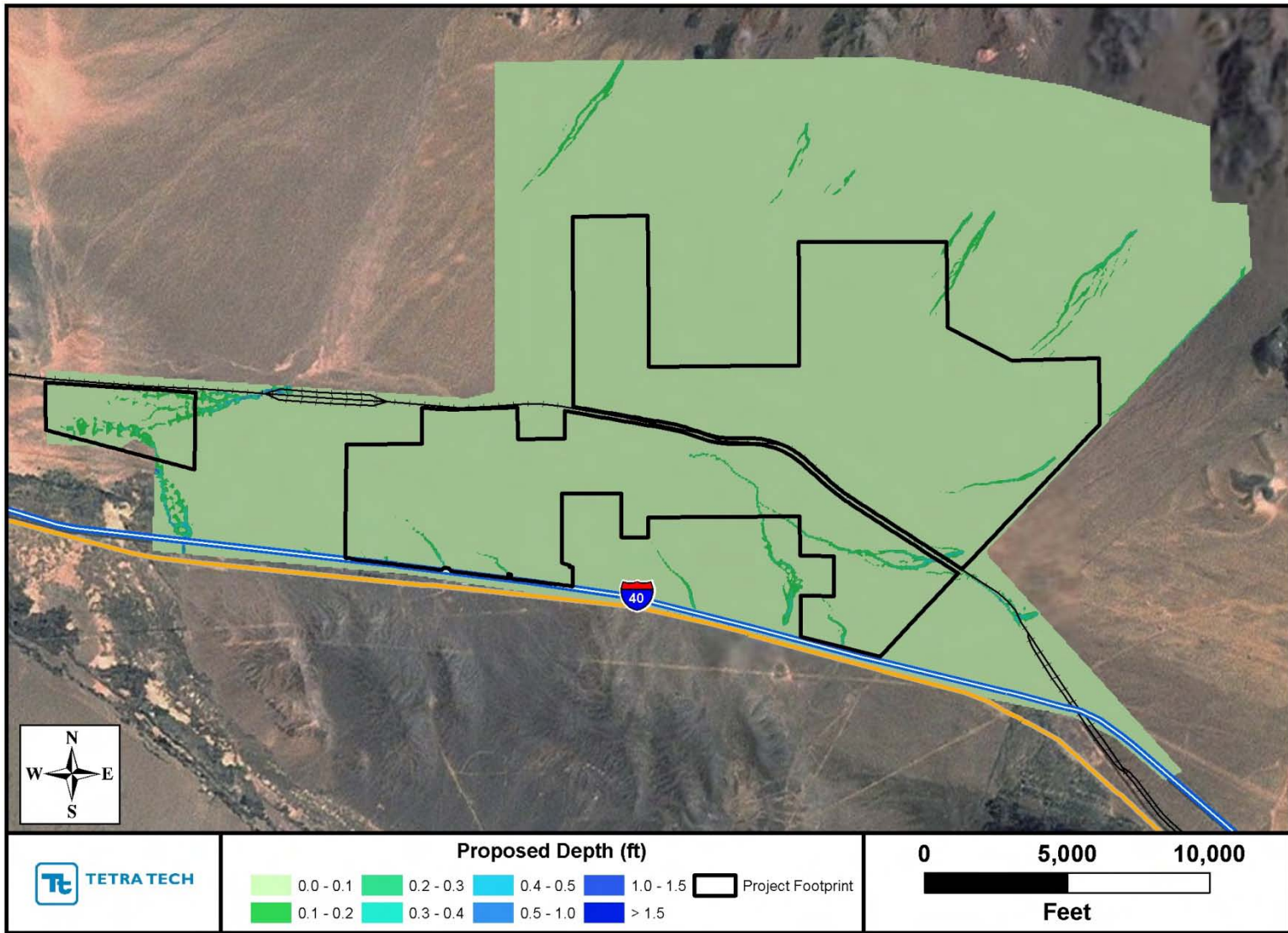
Maximum velocity during the 25-year, 24-hour storm.



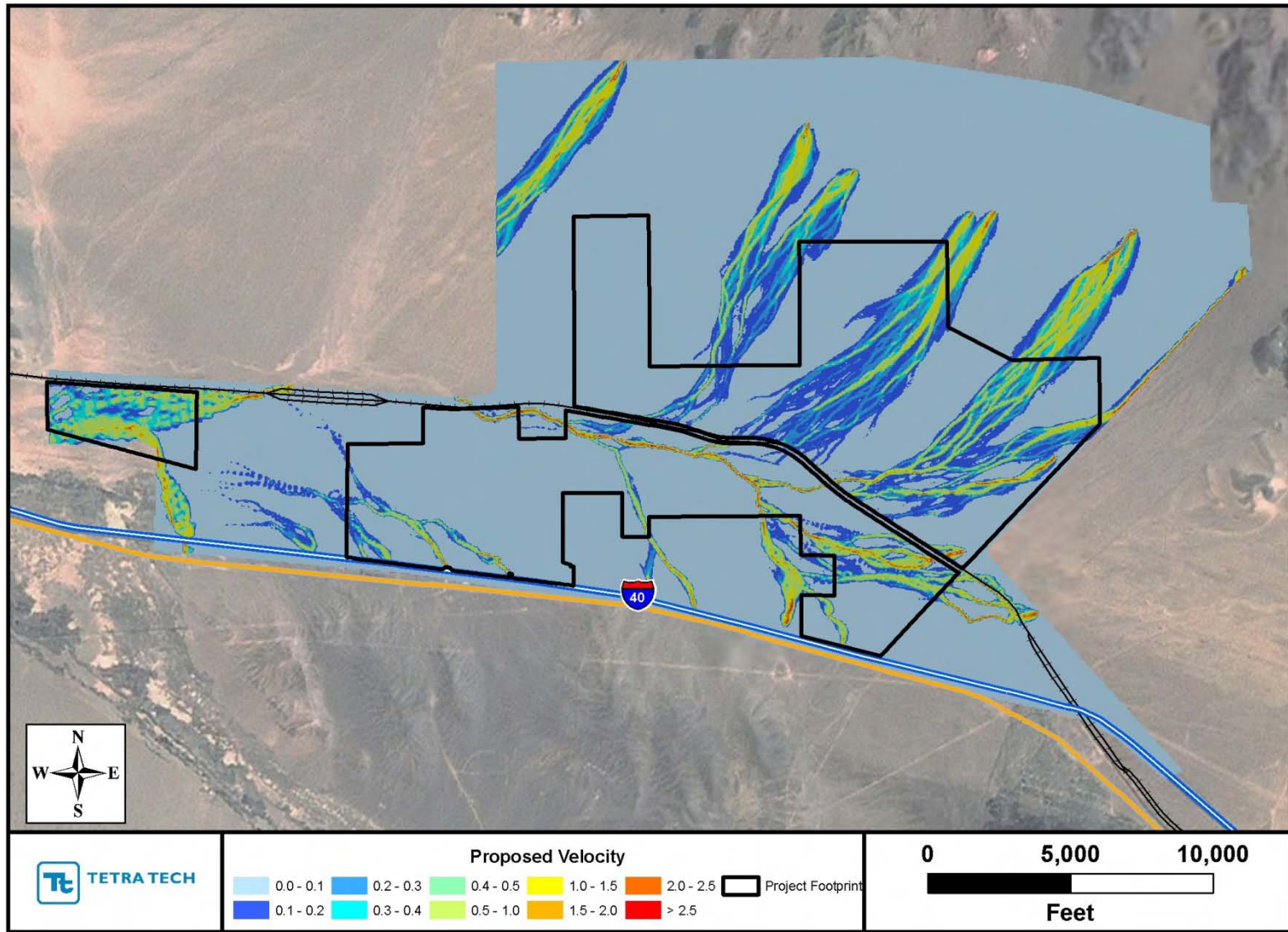
Maximum depths during the 10-year, 24-hour storm.



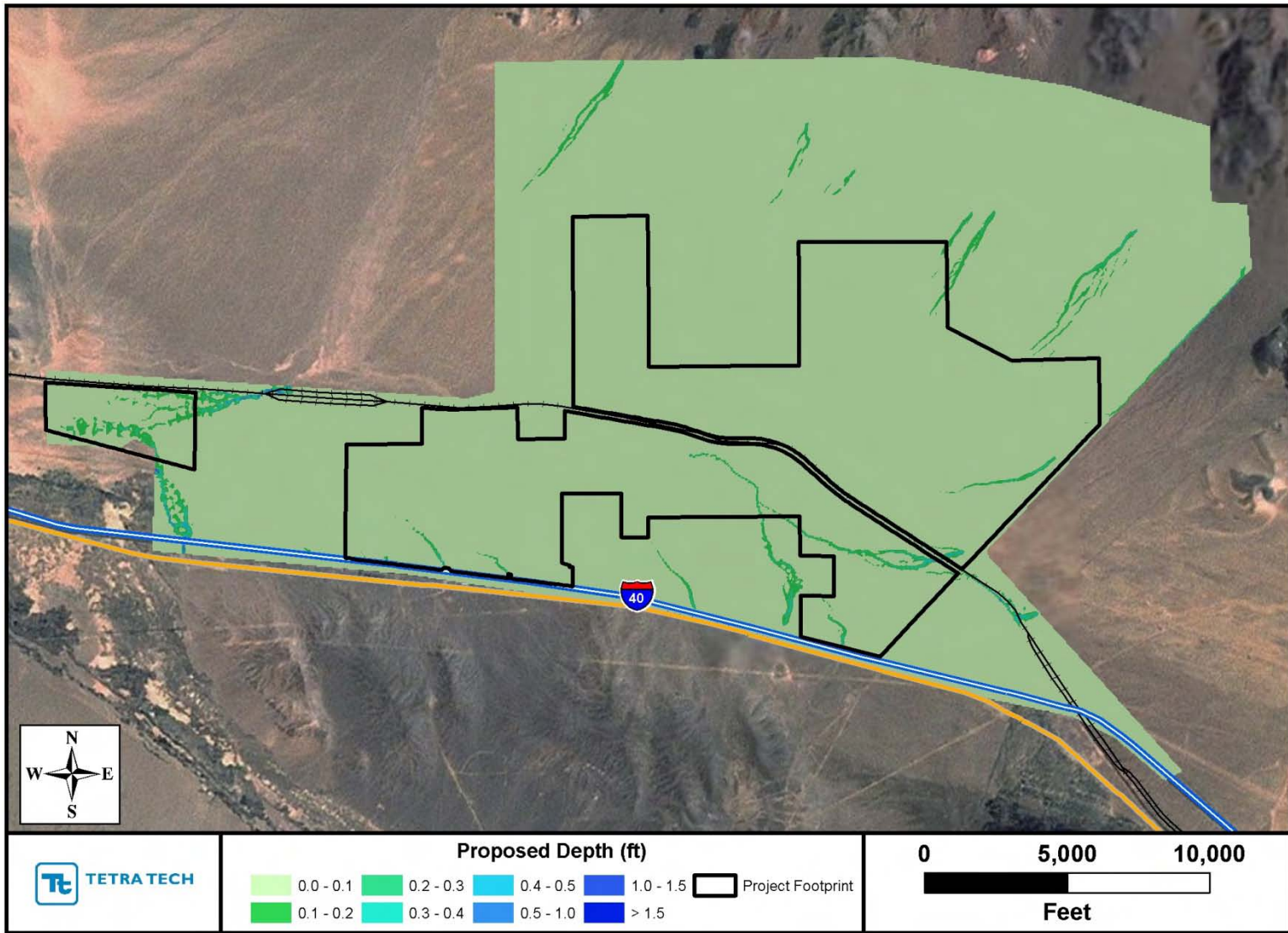
Maximum velocity during the 10-year, 24-hour storm.



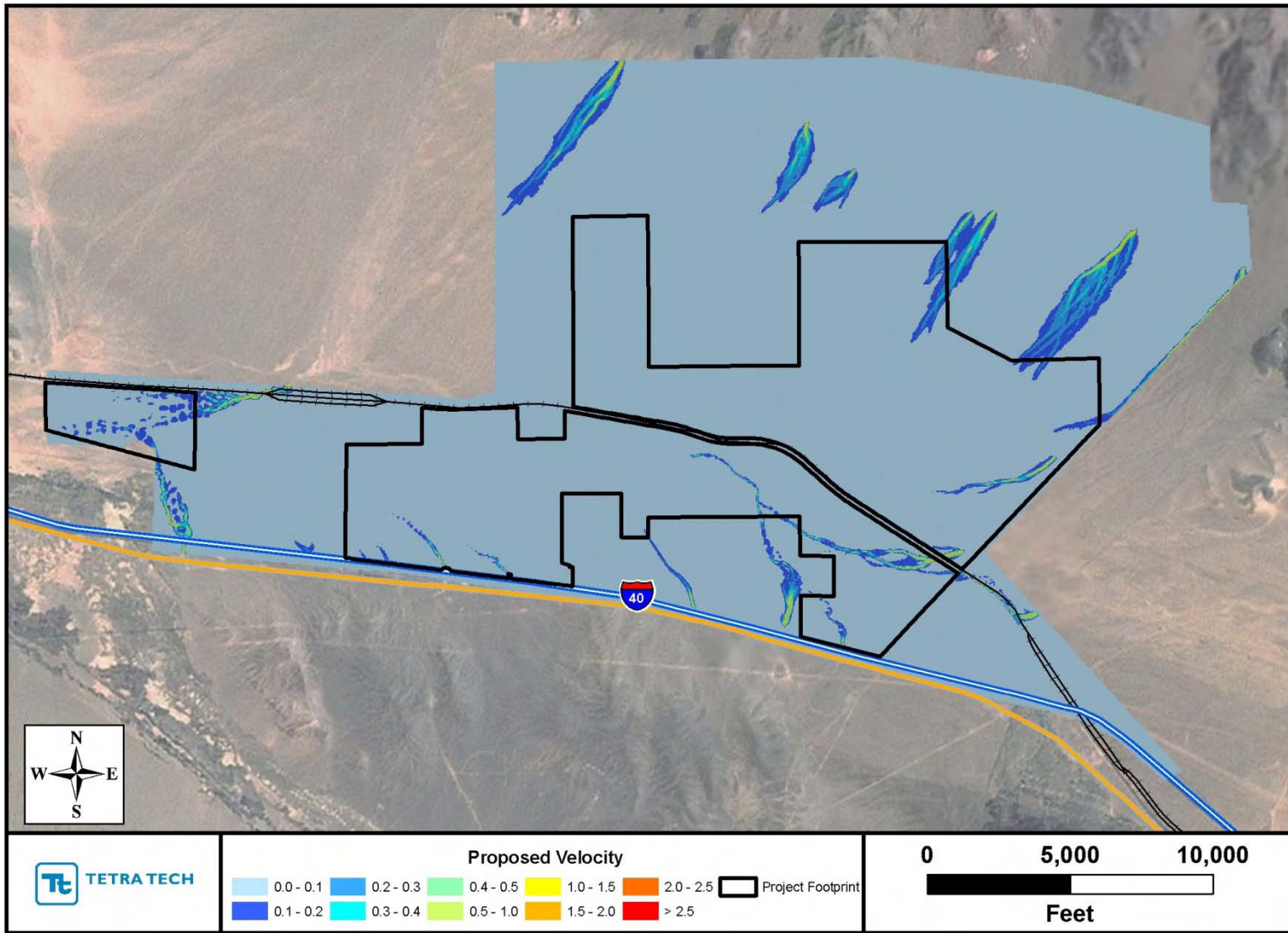
Maximum depths during the 5-year, 24-hour storm.



Maximum velocity during the 5-year, 24-hour storm.



Maximum depths during the 2-year, 24-hour storm.



Maximum velocity during the 2-year, 24-hour storm.



BEFORE THE ENERGY RESOURCES CONSERVATION AND DEVELOPMENT
COMMISSION OF THE STATE OF CALIFORNIA
1516 NINTH STREET, SACRAMENTO, CA 95814
1-800-822-6228 – WWW.ENERGY.CA.GOV

**FOR THE CALICO SOLAR PROJECT
AMENDMENT**

**Docket No. 08-AFC-13C
PROOF OF SERVICE
(Revised 8/1/2011)**

APPLICANT

Calico Solar, LLC
Daniel J. O'Shea
Managing Director
2600 10th Street, Suite 635
Berkeley, CA 94710
dano@kroadpower.com

Basin and Range Watch
Laura Cunningham,
Kevin Emmerich
P.O. Box 70
Beatty, NV 89003
e-mail service preferred
atomictoadranch@netzero.net

Newberry Community
Service District
c/o Wayne W. Weierbach
P.O. Box 206
Newberry Springs, CA 92365
e-mail service preferred
newberryCSD@gmail.com

CONSULTANT

URS Corporation
Angela Leiba
AFC Project Manager
4225 Executive Square, #1600
La Jolla, CA 92037
angela_leiba@URSCorp.com

California Unions for Reliable
Energy (CURE)
c/o: Tanya A. Gulesserian,
Marc D. Joseph
Adams Broadwell Joseph
& Cardozo
601 Gateway Boulevard,
Ste. 1000
South San Francisco, CA 94080
e-mail service preferred
tgulesserian@adamsbroadwell.com

Defenders of Wildlife
Kim Delfino, California Program Director
1303 J Street, Suite 270
Sacramento, California 95814
e-mail service preferred
kdelfino@defenders.org

APPLICANT'S COUNSEL

Allan J. Thompson
Attorney at Law
21 C Orinda Way #314
Orinda, CA 94563
allanori@comcast.net

Patrick C. Jackson
600 Darwood Avenue
San Dimas, CA 91773
e-mail service preferred
ochsjack@earthlink.net

Defenders of Wildlife
Jeff Aardahl, California Representative
46600 Old State Highway, Unit 13
Gualala, California 95445
e-mail service preferred
jaardahl@defenders.org

Bingham McCutchen, LLP
Ella Foley Gannon, Partner
Three Embarcadero Center
San Francisco, CA 94111
e-mail service preferred
ella.gannon@bingham.com

Sierra Club
Gloria D. Smith,
Travis Ritchie
85 Second Street, Second floor
San Francisco, CA 94105
e-mail service preferred
gloria.smith@sierraclub.org
travis.ritchie@sierraclub.org

BNSF Railroad
Cynthia Lea Burch,
Helen B. Kim,
Anne Alexander
Katten Muchin Rosenman LLP
2029 Century Park East, Suite 2700
Los Angeles, CA 90067-3012
cynthia.burch@kattenlaw.com
helen.kim@kattenlaw.com
anne.alexander@kattenlaw.com

INTERVENORS

Society for the Conservation of
Bighorn Sheep
Bob Burke, Gary Thomas
1980 East Main St., #50
Barstow, CA 92311
e-mail service preferred
cameracoordinator@sheepsociety.com

County of San Bernardino
Jean-Rene Basle, County Counsel
Bart W. Brizzee, Principal Assistant
County Counsel
385 N. Arrowhead Avenue, 4th Fl.
San Bernardino, CA 92415-0140

bbrizzee@cc.sbcounty.gov

**INTERESTED
AGENCIES/ENTITIES/PERSONS**

California ISO
e-recipient@caiso.com

BLM – Nevada State Office
Jim Stobaugh
P.O. Box 12000
Reno, NV 89520
jim_stobaugh@blm.gov

Bureau of Land Management
Joan Patrovsky, Specialist/
Project Manager
CDD-Barstow Field Office
2601 Barstow Road
Barstow, CA 92311
jpatrovs@blm.gov

California Department of
Fish & Game
Becky Jones
36431 41st Street East
Palmdale, CA 93552
dfgpalm@adelphia.net

BNSF Railroad
Steven A. Lamb
Katten Muchin Rosenman LLP
2029 Century Park East, Suite 2700
Los Angeles, CA 90067-3012
steven.lamb@kattenlaw.com

**ENERGY COMMISSION –
DECISIONMAKERS**

KAREN DOUGLAS
Commissioner and Presiding Member
kldougl@energy.state.ca.us

Galen Lemei
Adviser to Commissioner Douglas
glemei@energy.state.ca.us

ROBERT B. WEISENMILLER
Chairman and Associate Member
rweisenm@energy.state.ca.us

Eileen Allen
Adviser to Chairman Weisenmiller
eallen@energy.state.ca.us

Kourtney Vaccaro
Hearing Officer
kvaccaro@energy.state.ca.us

ENERGY COMMISSION STAFF

Kerry Willis
Staff Counsel
e-mail service preferred
kwillis@energy.state.ca.us

Stephen Adams
Co-Staff Counsel
e-mail service preferred
sadams@energy.state.ca.us

Craig Hoffman
Project Manager
e-mail service preferred
choffman@energy.state.ca.us

Caryn Holmes
e-mail service preferred
cholmes@energy.state.ca.us

**ENERGY COMMISSION – PUBLIC
ADVISER**

Jennifer Jennings
Public Adviser
e-mail service preferred
publicadviser@energy.state.ca.us

DECLARATION OF SERVICE

I, Doug Larson, declare that on September 12, 2011, I served by U.S. mail and filed copies of the attached Calico Solar Project Geomorphic Report. The original document, filed with the Docket Unit, is accompanied by a copy of the most recent Proof of Service list, located on the web page for this project at:

[www.energy.ca.gov/sitingcases/calicosolar/compliance/index.html].

The documents have been sent to both the other parties in this proceeding (as shown on the Proof of Service list) and to the Commission's Docket Unit, in the following manner:

(Check all that Apply)

FOR SERVICE TO ALL OTHER PARTIES:

- sent electronically to all email addresses on the Proof of Service list;
- by personal delivery;
- by delivering on this date, for mailing with the United States Postal Service first-class mail, or other equivalent delivery service, with postage thereon fully prepaid, to the name and address of the person served, for mailing that same day in the ordinary course of business; that the envelope was sealed and placed for collection and mailing on that date.

AND

FOR FILING WITH THE ENERGY COMMISSION:

- sending one electronic copy via e-mail and one original paper copy and with enclosures provided on two sets of three DVD formatted discs, mailed by first class mail, or other equivalent delivery service, with postage prepaid, to the address below;

OR

- depositing in the mail an original and 12 paper copies, as follows:

CALIFORNIA ENERGY COMMISSION

Attn: Docket No. 08-AFC-13C
1516 Ninth Street, MS-4
Sacramento, CA 95814-5512
docket@energy.state.ca.us

I declare under penalty of perjury that the foregoing is true and correct, that I am employed in the county where this mailing occurred, and that I am over the age of 18 years and not a party to the proceeding



Doug Larson, Paralegal
Bingham McCutchen LLP